# Reduced function of the RNA export factor, *Nxt1*, in *Drosophila* causes muscle degeneration and lowers expression of genes with long introns and circular RNA.

Kevin van der Graaf[1], Katia Jindrich, Robert Mitchell and Helen White-Cooper*

School of Biosciences, Cardiff University, United Kingdom

1, current address: Department of BioSciences, Rice University, Houston, TX 77005, USA.

* Corresponding author, E-mail: white-cooperh@cardiff.ac.uk

Short title "RNA export factor Nxt1 ensures muscle integrity and maintenance"

## Abstract

The RNA export pathway is essential for export-competent mRNAs to pass from the nucleus into the cytoplasm, and thus is essential for protein production and normal function of cells. *Drosophila* with partial loss of function of *Nxt1*, a core factor in the pathway, show reduced viability and male and female sterility. The male sterility has previously been shown to be caused by defects in testis-specific gene expression, particularly of genes without introns. Here we describe a specific defect in growth and maintenance of the larval muscles, leading to muscle degeneration in *Nxt1* mutants. RNA-seq revealed reduced expression of many mRNAs, particularly from genes with long introns in *Nxt1* mutant muscles. We further determined that circRNAs derived from these same genes are also reduced in the mutants. Despite this, the degeneration was rescued by increased expression in muscles of a single gene, the costamere component *tn (abba)*. This is the first report of a specific role for the RNA export pathway gene *Nxt1* in muscle integrity. Our data on *Nxt1* links the mRNA export pathway to a global role in expression of mRNA and circRNA from common precursor genes, *in vivo.*

## Author summary

In eukaryotic cells, the DNA encoding instructions for protein synthesis is located in the nucleus. It is transcribed into pre-mRNA, which is processed at both ends and spliced to remove internal spacer regions (introns) to generate mRNA. This mRNA is then transported to the cytoplasm by the mRNA export pathway via nuclear pores, and then used as a template for protein synthesis. We have previously shown that reduction in activity of a specific protein in the mRNA export pathway, Nxt1, has an additional role in testis-specific transcription. Here we describe a further role for this protein specifically in gene expression, particularly of genes with long introns and circular RNAs, and in muscle maintenance. *Drosophila* larvae with reduced Nxt1 activity have normal muscle pattern when they are small, but show muscular atrophy and degeneration as they grow, resulting in significant defects in their movement speed. We discovered that expression of many genes is reduced in the *Nxt1* mutant larvae, but that restoring the expression of just one of these, *abba*, the *Drosophila* homologue of *Trim32* (a human gene involved in muscular dystrophy) is capable of preventing the muscle degeneration. Our data provide a new insight into how defects in generally acting cellular factors can lead to specific defects similar to human diseases.

## Introduction

The formation, growth and maintenance of the musculature is critical for normal animal function, and defects in these processes can lead to impaired mobility, shorter lifespan or early lethality. The somatic muscular tissue of *Drosophila melanogaster* is generated via a highly regulated developmental programme in embryogenesis, such that the first instar larva contains a stereotyped pattern of muscles [1]. The abdominal A2-A7 segments each contain 30 muscles on each side of the animal, each with defined size, shape, position and attachment sites. Each muscle is a single multinucleated cell, derived from fusion of muscle founder cells with fusion competent myoblasts (reviewed in [2]). Very severe defects in embryonic myogenesis result in a failure of the embryo to hatch; less severe defects in the development of the muscle pattern or in muscle function can result in animals with impaired mobility. During larval stages, no new cells are added but the muscles grow extensively by addition of new myofibrils, particularly during the final larval instar (reviewed in [3]).

Normal muscle function is essential during pupariation, and defects in larval muscles can lead to lethality at this stage. About 12 hours before pupariation, a pulse of ecdysone triggers the larvae to stop feeding and move out of the food. About 6-10 hours later they stop moving, contract longitudinally, evert their spiracles and become a white pre-pupa. Three hours later the prepupa contracts from the anterior partially withdrawing the anterior tracheal lining [4]. At this stage, an air bubble forms in the abdominal cavity. The bubble gradually increases in size and the abdominal tissue is forced against the body wall. One hour later, the prepupa becomes separated from the puparium due to the secretion of the prepupal cuticle. The air bubble migrates to the anterior by

abdominal muscular contractions, creating space inside the puparium to evert the head, which up to this point has been developing internally [4]. Orchestration of these events requires pristine muscle function.

Regulation of gene expression is important for the normal development and functioning of organelles, cells, tissues and the whole organism. Regulation of mRNA expression depends on transcriptional regulatory processes, such as transcription factor and repressor binding, that influence the ability of RNA polymerase to bind to the promoter site and carry out transcription. Post-transcriptional regulation of RNA adds additional layers of potential control, both in the nucleus and after mRNA export to the cytoplasm. Within the nucleus, critical processing and control points include (alternative) splicing of exons and association of the RNA with mRNA nuclear export factors. The passage of the mRNA transcripts to the cytoplasm requires the export factors associated with the transcript to be recognized by receptors in the interior of the pores (reviewed in [5]). In *D. melanogaster*, the association of nascent RNA with export factors occurs co-transcriptionally and involves first the binding of hnRNPs to the transcript, then recruitment of the THO export complex, and finally recruitment of a heterodimer of Nxf1/Nxt1. The THO complex interacts with UAP56 and REF to form transcription-export complex (TREX) [6]. During the recruitment of Nxf1/Nxt1, export factors such as UAP56 and THO complex are displaced from the RNA. Splicing of pre-mRNAs not only results in removal of the intron sequence from the transcript, but also results in the deposition of a protein complex, the Exon Junction Complex (EJC) 5' of the splice junction. The EJC has many regulatory roles, including acting to help recruit the RNA export components, and thus facilitates nuclear export of correctly processed mRNAs (reviewed in [7]).

While most pre-mRNAs are spliced to generate linear mRNA molecules, a small proportion of generate circular RNAs (circRNAs) by splicosome-dependent back splicing of segments of primary transcripts (reviewed in [8, 9]). The 3' end of an exon splices to the 5' end of the same exon, or to a further upstream splice acceptor site in some cases. The production of circRNA depends on alternative transcript processing; typically, the exon that is circularized is not subject to conventional alternative splicing, but is flanked by relatively long introns [10]. Modulation of transcription rate and splicing rate both affect the relative efficiency of forward and back splicing events, and thus can alter the expression level or ratio of the alternative products [11, 12]. Once formed, circRNAs are relatively stable, and, while typically of relatively low abundance, they can accumulate to levels equal to or even exceeding that of the mRNA(s) derived from the same gene. Analysis of total RNA sequencing data has revealed at least 2500 circRNAs expressed in *Drosophila melanogaster* [13]. CircRNAs are particularly abundant in neural tissue, but all analysed tissues express some circRNAs [13]. CircRNAs have been shown to have a variety of

106 roles *in vivo*, including acting as miRNA sponges, protein sponges, protein scaffolders and being
107 translated (reviewed in [8, 9]).

108

109 Human muscular dystrophies are a group of inherited genetic conditions that cause muscles to
110 weaken, leading to an increasing level of disability. Some, such as Duchenne muscular dystrophy
111 and limb girdle muscular dystrophy 2H, are caused by mutations in genes encoding muscle
112 structural proteins (*dystrophin* and *Trim32* respectively) [14, 15], while others, like myotonic
113 dystrophy, are caused by defects in RNA metabolism (Reviewed in [16, 17]). For example DM1
114 myotonic dystrophy, a trinucleotide repeat in the 3' UTR of the *DMPK* gene results in sequestration
115 of the splicing regulator MBNL1, and this in turn causes defects in muscle gene expression,
116 particularly alteration of splicing patterns. Interestingly, both MBNL1 and *muscleblind* (*mbl*), the
117 *Drosophila* orthologue of MBNL1, produce abundant circular RNAs [11]. Moreover, Mbl protein is
118 implicated in regulation of production of its own circRNA [11], although the MBNL1 circRNA has
119 not yet been implicated in myotonic dystrophy [18].

120

121 We have previously described a role for Nxt1 in regulation of transcription in *Drosophila* testes,
122 indicating that the level of this gene product is critical for processes beyond its known role in
123 mRNA nuclear export [19]. Here we describe a specific role for Nxt1 in the maintenance of larval
124 muscles. Specifically, *Nxt1* partial loss of function animals showed muscle degeneration during the
125 extensive growth associated with the final larval instar stage. We demonstrate that this is probably
126 due to its role in the RNA export pathway as knock down of other RNA export factors caused a
127 similar muscle degeneration phenotype. We found that normal expression of many genes,
128 particularly those with long introns that are sources of circRNAs, requires *Nxt1*. We discovered that
129 both the mRNA and circRNA products of these *Nxt1*-responsive genes are reduced in mutants,
130 although the nascent transcripts of these genes are produced at normal levels. Despite the large
131 number of altered transcripts we were able to rescue the muscle degeneration of *Nxt1* mutants, but
132 not the pupal lethality, by expression of the *Drosophila* homologue of *Trim32*, *tn (abba)*, in
133 muscles. Together, our data indicate an unexpected role for *Nxt1* in post-transcriptional regulation
134 of many genes and circRNA splice products, and show that this RNA export protein is essential for
135 muscle maintenance.

136

137

138

139

140 **Results**

141 **Nxt1 pupae have a distinctive curved shape, uneverted spiracles and fail head eversion**

142 We have previously described that *Nxt1*$^{z2-0488}$ / *Nxt1*$^{DG05102}$ transheterozygotes are male and female
143 sterile, but also have significantly reduced viability [19]. *Nxt1*$^{DG05102}$ is a null allele caused by a P-
144 element insertion into the coding sequence of the gene, while *Nxt1*$^{z2-0488}$ is a hypomorphic allele
145 that disrupts a hydrogen bonding network in the core of the protein thus reducing protein stability
146 [19]. Many *Nxt1*$^{z2-0488}$ / *Nxt1*$^{DG05102}$ transheterozygote pupae had a curved shape and uneverted
147 spiracles (Figure 1A). To quantify this morphological defect we measured the axial ratios from the
148 pupa by measuring the length (excluding the posterior and anterior spiracles) and width. This
149 confirmed that the mutant pupae were significantly longer and thinner than wild type (t-test, p= 1e-
150 08). Scanning electron microscopy (SEM) revealed that the surface structure of the pupal case
151 was similar between mutant and wild type (Figure 1C-E) while in Nxt1 trans-heterozygotes, 50%
152 larvae (N=36) had uneverted anterior spiracles (Figure 1E'').

153 We have also previously reported that the *Nxt1*$^{z2-0488}$ / *Nxt1*$^{DG05102}$ transheterozygote pupae show
154 failure in head eversion [19]. Air bubble formation and migration is implicated in head eversion and
155 therefore the viability of the pupa. To analyse this process we filmed *w*$^{1118}$ and *Nxt1*$^{z2-0488}$ / *Nxt1*
156 $^{DG05102}$ trans-heterozygote pre-pupae and for 15 hours to observe the air bubble; a typical series is
157 shown. (Supplementary Figure 1) In wild type controls, head eversion occurs at around 12 hours
158 into the pupa phase (Supplementary Figure 1M). Before the head eversion occurred, there was a
159 dramatic period of muscular contractions, as the posterior of the larva wriggled then contracted
160 towards the anterior. At the same time as head eversion, the whole larva body wriggled back within
161 the pupal case to reach the posterior end. The air bubble formed normally in the mutants, and was
162 faintly visible from 0h after pupa formation (APF), growing in size over the next few hours
163 (Supplementary Figure 1A). However, air bubble migration stalled by 8h APF (Supplementary
164 Figure 1I); it remained in the middle of the pupa until 11h APF (Supplementary Figure 1J-M) before
165 disappearing and leaving an empty space at the posterior of the pupa body (Supplementary Figure
166 1N-P). No head eversion was seen in this mutant pupa (Supplementary Figure 1M).

167 Crosses of *Nxt1*$^{DG05102}$/*CyO, Act-GFP* to *Nxt1*$^{Z2-0488}$/ *CyO, Act-GFP* did not reveal the expected
168 Mendelian ratios of 1:2 (Nxt1 trans-heterozygotes: *CyO, Act-GFP;* note *CyO, Act-GFP*
169 homozygotes are lethal). Instead, the observed ratio was 1:10. We assessed the progression of
170 pupal development at four time points (24h, 48h, 72h and 96h pupa), and the number of viable
171 adults. Only about 20% (N=182) of the Nxt1 trans-heterozygote pupae survived through to
172 adulthood, compared to 90% (N= 287) viability for control *w*$^{1118}$ pupae (Supplementary Figure 2).
173 The *Nxt1*$^{DG05102}$/+ showed a slight reduction to pupa viability (60% (N= 211); Supplementary Figure
174 2). Head eversion occurs roughly 12 hours into the pupa stage. Pupa metamorphosis continued
175 (such as body, bristles and wings) in *Nxt1* trans-heterozygotes where most pupa did not have head
176 eversion. The consequence of no head eversion was seen between 48-96 hours into
177 metamorphosis as development stopped abruptly, and the pupae blackened.

178

179 **Ecdysone-responsive gene expression is not affected in *Nxt1* mutants**

180 The air bubble phenotype suggests that there are defects in the function of the larval/pupal
181 abdominal muscles, or in the developmental regulation of their function at this stage. Ecdysone
182 coordinates tissue-specific morphogenetic changes by several pulses throughout the *Drosophila*
183 development (reviewed in [20]). A high concentration pulse is observed immediately preceding the
184 larva-pupa transition, and this pulse is essential to trigger the muscular contractions on pupariation
185 and in the pre-pupa. To understand if a transcriptional defect downstream of ecdysone signalling is
186 responsible for the phenotype, in a manner analogous to the role for Nxt1 in regulation of testis-
187 specific transcripts dependent on the transcriptional activation complex tMAC [19], we performed
188 RNA sequencing of pooled whole larvae before (wandering larvae), during (stationary larvae), and
189 after (white prepupae) the pulse of ecdysone.

190 We extracted the expression data for known ecdysone-responsive genes [21]. Out of 87 ecdysone-
191 responsive genes, only four were mildly mis-regulated (Supplementary Table 1). Mutants of these
192 four genes do not show an air bubble phenotype [22, 23], therefore, it is unlikely that failure of
193 expression of ecdysone-responsive genes is responsible for the air bubble phenotype in Nxt1
194 trans-heterozygotes.

195

196 **Muscle degeneration occurs in *Nxt1* mutant larvae**

197 To determine whether the defects seen in pupal and pre-pupal stages in *Nxt1* mutants are due to
198 muscular defects, we characterised the structure and function of muscles in the larval stages. A
199 larval movement assay was used to track 1$^{st}$, 2$^{nd}$, and 3$^{rd}$ instar larvae to compare their speed
200 between stages and between $w^{1118}$ and Nxt1 trans-heterozygotes. Larvae were tracked on an agar
201 plate with a control odour on each side (Figure 2A and B). There was no significant difference in
202 the average speed of mutant larvae compared to wild type at either 1$^{st}$ or 2$^{nd}$ instar stage.
203 Normally, wild type 3$^{rd}$ instar larvae travel up to 5x faster than 2$^{nd}$ instars (Figure 2F). In contrast,
204 Nxt1 trans-heterozygous 3$^{rd}$ instar larvae were significantly slower than control animals (Figure
205 2C), indeed, they were no faster than 2$^{nd}$ instar larvae (Figure 2G), despite being much larger.

206 To investigate the muscle structure in the mutant animals we stained of 3$^{rd}$ instar larval body wall
207 muscles with phalloidin which labels F-actin. In *Drosophila* larvae, each of the abdominal
208 hemisegments A2-A7 has a stereotypical pattern of 30 different muscles [1]. This pattern was
209 clearly observed in the wild type (Figure 3A and C), however, $Nxt1^{z2\text{-}0488}$ / $Nxt1^{DG05102}$ trans-
210 heterozygotes showed clear signs of muscle degeneration (Figure 3B, D and E). Defects seen
211 were variable, and included thinner muscles, fibre splits and torn muscles (Figure 3F-K). We
212 counted the number and nature of defective muscles in 8 hemisegments of 6 control and 6 mutant
213 third instar larvae and categorized the nature of the defects. Defects seen in the mutants were

214 variable and included thinner muscles (15%), loss of sarcomeric structure (22%), degenerating
215 muscles (77%), torn muscles (8%); all control animals had no defects.

216 In addition to the gross morphological defects, *Nxt1*$^{z2\text{-}0488}$ / *Nxt1*$^{DG05102}$ trans-heterozygote mutant
217 animals also sometimes had defects in internal muscle structure. Normal muscle sarcomere
218 structure consists of thick and thin filaments, and phalloidin staining of actin reveals this structure
219 by labelling the thin filaments in the sarcomere (Figure 4A). For Nxt1 trans-heterozygotes, the
220 sarcomere structure was compromised in 22% of the muscles examined. These muscles showed
221 more uniform phalloidin staining indicating weak or absent differentiation of thin vs thick filaments
222 (Figure 4C). This muscle degeneration and sarcomere structure defect phenotype was not fully
223 penetrant, and some Nxt1 trans-heterozygotes had more normal sarcomere structure and less
224 obvious muscle degeneration. This is consistent with the finding that about 20% of the mutant third
225 instar larvae are able to develop to adulthood (Figure 4B). We analysed muscles from first (N=8)
226 and second (N=10) instars with phalloidin staining. This revealed that earlier stage larvae have a
227 normal musculature, and thus that the defects are due to degeneration rather than a
228 developmental defect.

229 To confirm that the muscle phenotype observed was due to defects in *Nxt1* rather than being a
230 non-specific effect, we used Mef2-Gal4 to drive UAS-RNAi expression specifically in muscles. We
231 combined this with UAS-dicer and high induction temperature to achieve a strong knockdown of
232 the transcript. Both RNAi lines 103146 (chromosome 2) and 52631 (chromosome 3) had
233 previously been shown to effectively knock down *Nxt1* and phenocopy the mutant phenotype in
234 spermatocytes [19]. Phalloidin staining of these 2$^{nd}$ instar larvae showed extensive muscle
235 degeneration (Figure 5). When the temperature was 25$^{o}$C for embryonic development, with a shift
236 to 29$^{o}$C after hatching, line 52631 still induced early 2$^{nd}$ instar lethality, while 103146 gave a
237 weaker phenotype of third instar larval lethality, very similar to the *Nxt1*$^{z2\text{-}0488}$ / *Nxt1*$^{DG05102}$ trans-
238 heterozygote hypomorphic condition. This indicates that knock down of *Nxt1* specifically in
239 muscles is able to phenocopy the *Nxt1* mutant situation, and shows that the degeneration is due to
240 reduction in *Nxt1* activity in muscles.

241 We expressed GFP-Nxt1 via the UAS-gal4 system both exclusively in muscles at a high level (with
242 mef2-gal4>UAS-GFP-*Nxt1*) and ubiquitously at a lower level (with arm-gal4>UAS-GFP-*Nxt1*) in
243 *Nxt1* trans-heterozygotes. High level, muscle-specific, GFP-Nxt1 expression was able to partially
244 rescue muscle integrity in *Nxt1* trans-heterozygotes (~13-26% with two 47% outliers (N= 10)
245 Figure 6C) and partially rescue the pupa lethality (~40% (N= 186); Figure 6A). On average, the
246 axial ratios were similar to wild type, albeit more variable (Figure 6B). Finally, mobility was
247 increased compared to *Nxt1* trans-heterozygotes, but was still significantly reduced compared to
248 wild type (Student's t-test * $p<0.05$; Figure 6D). Lower level ubiquitous expression of GFP-*Nxt1* in
249 Nxt1 trans-heterozygotes resulted in improved, but not fully rescued muscle integrity (~3-33%

damage with one 73% outlier (N= 9), increased the pupa viability (~75% (N= 163)) and increased larval mobility. The axial ratios were similar to wild type (Figure 6B).

## Muscle degeneration is associated with larval growth

During the last instar phase, larvae will grow substantially compared to earlier instars. Larvae removed from the food 70 hours after egg laying do not grow, but still crawl until the normal time for pupation (~112 hours AEL) and may survive through to adulthood, generating very small flies [24]. Larvae at 70 hours AEL are late 2$^{nd}$, or early 3$^{rd}$ instars.

To test whether growth or use (movement) is implicated in the muscle degeneration in *Nxt1* mutants, we fed ~60 larvae for 70-73 hours then removed them from the food. 14-25% of the larvae (removed from food at 70-73 hr) were able to pupate although less than 5% of those pupae were able to emerge as adults. We simultaneously examined ~60 of the Nxt1 trans-heterozygote larvae that were starved from 70-hour AEL and found, that only a few larvae pupated and none emerged as adults (similar to $w^{1118}$). The pupae that formed had everted spiracles (Figure 7A) and resembled the wild type controls. Interestingly, the larvae that failed to pupate were able to survive for several additional days as larvae before dying. Nxt1 trans-heterozygote larvae were dissected four days after they were removed from the food, and were stained with phalloidin. For all larvae (n=10), no muscle degeneration was observed (Figure 7B). These larvae had been moving normally and thus using their body wall muscles for the four days of starvation. The lack of abnormalities in these animals indicates that the muscle growth, or high levels of force generation associated with third instar larval movement, rather than use per se, is critical for degeneration in *Nxt1* mutants.

## Other RNA export factors are also required for maintenance of muscle integrity in *Drosophila* larvae.

*Nxt1*'s well characterised function is in the RNA export pathway. To determine whether the muscle degeneration phenotype is caused by defects in this pathway, we assessed the phenotype of knock down of other RNA export pathway genes. We used arm-gal4, to drive RNAi hairpin constructs targeted against *thoc5, sbr (Nxf1), Ref1* and *Hel25E (UAP56)*. This is designed to reduce, but not complete eliminate the RNAi target gene expression throughout the larva. As a positive control we used RNAi against *Nxt1*, and as a negative control we used both $w^{1118}$ and arm-gal4 alone. RNAi against *Hel25E* caused early larval lethality, even when tested at lower temperature, so we were not able to assess the role of this gene in muscle maintenance. For all the other genotypes, we assayed third instar muscle integrity with phalloidin staining. Knock down of these RNA export pathway components caused a similar phenotype to knock down of *Nxt1*, with muscle thinning and tearing apparent (Figure 8B-E'). Control larvae (arm-gal4 alone and $w^{1118}$) had normal musculature (Figure 8A and A' and data not shown). This indicates that the role of *Nxt1* in

287 muscle maintenance is most likely to be attributable to its role in the RNA export pathway rather
288 than an un-related function.

289

290 **Genes with long introns that also produce circRNAs are sensitive to the loss of Nxt1**

291 The known role of *Nxt1* in RNA export and transcriptional control suggested that the muscle
292 phenotype could be due to transcriptional or post-transcriptional defects in gene expression. To
293 identify somatically expressed differentially expressed genes, we performed RNA sequencing from
294 stationary third instar larval carcasses (comprising primarily muscle and cuticle). Each genotype
295 ($w^{1118}$ and Nxt1 trans-heterozygotes) was analysed in triplicate. 572 genes were 2x or more up-
296 regulated in mutant compared to wild type, while 1340 genes were similarly down-regulated. The
297 numbers of genes up- and down-regulated at different fold change cut offs are shown in Table 1.
298 To investigate properties of differentially expressed genes we focussed on aspects of RNA
299 processing in the nucleus, and particularly intron length. Nxt1 is important for mRNA export, is
300 recruited indirectly by EJC to spliced transcripts [25], and mutations in the EJC can cause reduced
301 accumulation of transcripts with long introns [26]. In contrast, in *Nxt1* trans-heterozygote testes,
302 transcripts from short and intron-less genes were dramatically reduced. In *Nxt1* trans-heterozygote
303 testes, addition of at least one intron to a down-regulated gene resulted in increased transcript
304 production [19]. We initially analysed the total intron length, number of introns and smallest/largest
305 intron. This revealed that, in direct contrast to the situation in testes, genes down-regulated in *Nxt1*
306 mutant carcass had more introns and a higher total intron length than non-differentially expressed
307 genes, while up-regulated genes had fewer introns and a lower total intron length than the genes
308 that were not differentially expressed (Mann-Whitney test p-value $<0.05$, except for 16-fold up
309 regulated (p value of 0.16)); (Table 1 and Figure 9). We extended the analysis by also looking at
310 the gene length and shortest/longest transcripts (Table 2). Again, a clear trend showed that down-
311 regulated genes had longer median mRNA length and up-regulated genes had shorter median
312 mRNA length when compared to non-differentially expressed genes (Mann-Whitney $p<0.05$; Table
313 2). Finally, the genes down regulated in *Nxt1* mutants produced more mRNA isoforms than those
314 up regulated or not differentially expressed (Table 2). qRT-PCR for 12 genes with long introns
315 confirmed the down-regulation seen in the RNA sequencing data (Figure 10).

316 Long introns present a challenge to the spliceosome, and indeed some long introns are spliced as
317 several shorter fragments via recursive splicing [27]. Expression of most genes known to be
318 processed via recursive splicing was detected in our RNA-seq sample (112/116). Only 11 of these
319 were 8x or more down-regulated in the *Nxt1* mutants (34 were 4x or more down-regulated; Figure
320 9). We concluded that Nxt1 is unlikely to be required for recursive splicing *per se*, and considered
321 other aspects of genes with long introns.

322 Genes with long introns are sources of circular RNAs, with many circular RNA exons being flanked
323 by long introns [10]. We therefore compared the genes down-regulated in *Nxt1* muscles with lists

of genes known to produce circRNA transcripts [13], and found a striking overlap. 466 of the 567 genes 4x or more down-regulated in *Nxt1* muscles had at least one read consistent with a circRNA. 199 of these genes were in the higher confidence set associated with at least 10 circRNA reads. 57 of the 186 genes that were at least 8x down regulated in *Nxt1* muscles were also in the high confidence circRNA set. circRNAs are predominantly produced from genes that are known to have neuronal functions and whose expression is higher in nervous system, even when the analysis is performed on tissues outside the nervous system [13]. Consistent with this, embryonic expression pattern enrichment analysis via FlyMine revealed that the genes down-regulated in *Nxt1* muscles are indeed significantly enriched for expression in nervous-system (such as ventral nerve cord (p=1.13e-8), embryonic brain (p=3.06e-6)). We conclude that Nxt1 is important not only for the export of mRNAs but also for normal expression of mRNAs from genes with long introns, particularly those that produce circRNA products.

## CircRNAs are reduced in *Nxt1* mutants, but nascent transcripts are not

mRNAs and circRNAs are mutually exclusive products made from the same nascent transcript. If Nxt1 and the RNA export pathway controls the ratio between mRNAs and circRNAs, down regulation of Nxt1 would lead to an increase in circRNA products. Alternatively, Nxt1 could be implicated in the stability of the nascent RNA to ensure normal levels of both products, in which case we would expect a reduction in circRNA in target genes in the mutants. In a third model, Nxt1 could act after completion of splicing to stabilise just the mRNA; in this case the circRNA levels would be expected not to change in the mutant compared to wild type. To determine which of these models is most likely, we sequenced both total RNA (after depletion of the ribosomal RNAs) and circRNA (the RNAse R resistant fraction) from larval carcass samples from wild type and *Nxt1* transheterozygotes. The library preparation protocol did not include a selection for poly adenylated transcripts, and thus allowed us to examine pre-mRNA, both spliced and unspliced, as well as circRNA.

We first assessed the levels of circRNAs, focussing only on 336 structures identified in both genotypes with high confidence (backspliced reads identified in at least 2/3 replicates). This revealed that the majority of circRNAs are reduced in expression in *Nxt1* compared to wild type (Figure 11A-D). For these genes, pre-mRNA levels are unchanged in between wild type and mutants, while poly adenylated mRNA levels are reduced in mutants (Figure 11). Similarly, we found no difference between levels of spliced RNAs in when we assessed total RNA samples (Figure 11A-D). Thus, transcription of these genes, and splicing, is not affected in the mutants; however accumulation of poly adenylated transcript is reduced.

359 **Increased expression of *abba* rescues the muscle degeneration, but not semi-lethality**

360 Having identified a globlal defect in mRNA and circRNA for many genes, we were interested in
361 understanding how this leads to the muscle degeneration phenotype. The RNA expression of 13
362 known muscle-specific or muscle-enriched genes was analysed in our original whole larva mRNA-
363 seq data (Supplementary Table 2). Nine genes were more than 1.5-fold up regulated. *abba* (also
364 known as *thin* (*tn*)), the only gene significantly down regulated in this list, is an essential
365 TRIM/RBCC protein that maintains integrity of sarcomeric cytoarchitecture [28]. *abba* loss of
366 function mutations are lethal, with the larvae and pupae being long and thin and having muscle
367 degeneration [29]. *abba* is a large gene with several long introns, which also produces a circRNA
368 derived from circularisation of exon 7 (Figure 11E). The encoded protein has a RING finger, B-Box
369 & CC-domain and several NHL repeats (Figure 12A). qRT-PCR confirmed the reduction in *abba*
370 expression (n=30 larvae per sample; Figure 12). Levels of *abba* mRNA were highly variable
371 between individual stationary larvae (Figure 12) but significantly down in 9 out of 10 larvae, when
372 compared to a pool of 10 WT larvae (Figure 12B). *abba* has at least six isoforms with 13 exons in
373 its longest transcript and contains introns up to 4kb in length. We compared nascent (primers in
374 introns) versus spliced (primers in adjacent exons) abba transcript expression by Q-RT-PCR. Four
375 different regions were selected that would target as many isoforms as possible (Supplementary
376 Figure 3A). Consistent with our total RNA sequencing results, all regions throughout *abba* had
377 similar expression of nascent transcript in mutant compared to control animals, but the levels of
378 spliced transcript were reduced in mutants compared to control (Supplementary Figure 3B). Thus,
379 loss of *Nxt1* does not impact on *abba* transcription, but Nxt1 is important for normal accumulation
380 of the processed mRNA.

381

382 To determine whether reduction in the expression of *abba* was implicated in the mutant phenotype,
383 we used a UAS-*abba*$^{\text{full length (fl)}}$ cDNA construct (kindly gifted by Hanh T. Nguyen; hereafter referred
384 to as UAS-*abba*) and expressed it under the muscle specific driver mef2-gal4 in the *Nxt1* trans-
385 heterozygote background. Staining of the muscles of these larvae with phalloidin, showed that
386 muscle degeneration was fully rescued in 12 out of 16 animals and partially in the other four
387 (Figure 12C). qRT-PCR of individual stationary larvae showed again high variability between
388 individuals, but 8 out of 10 had *abba* expression equal to or exceeding that seen in wild type
389 (Figure 12D).

390 This result is surprising given the large number of genes whose expression is altered in the mutant
391 larvae. We therefore examined the ability of these animals to survive to adulthood and found that
392 the lethality was not rescued (22%; N=187). These genetic rescue experiments indicate that the
393 muscle defect in *Nxt1* mutant larvae is primarily due to the reduction in *abba* mRNA expression.
394 However, the pupal lethality of most *Nxt1* transheterozygotes is not solely caused by the muscular

395 degeneration, and reduced expression of other target genes is likely associated with reduction in
396 the viability of the animal.

397

398 ## Discussion

399 ### Reduction in Nxt1 function causes muscle degeneration

400 Nxt1 is primarily known for its role in the RNA export pathway. Nxt1 binds to Nxf1, which interacts
401 with the nuclear pore complex for exporting mRNA to the cytoplasm [30]. Reducing Nxt1 protein
402 level, reduces the Nxt1-Nxf1 dimer and without Nxt1, Nxf1 interacts less effectively with the
403 nuclear pore complex [31]. Since most mRNAs are exported via the Nxt1-Nxf1 route, it is expected
404 that many transcripts will be affected, and indeed this is what is seen in tissue culture cells [30].
405 Consistent with this, homozygotes of the null *Nxt1* allele are embryonic lethal. The hypomorphic
406 allele we have used causes reduced protein stability [19], but retains sufficient Nxt1 activity, even
407 when in trans to a null allele, to support mRNA export, and thus allows us to explore other
408 functions of this protein. Intriguingly, the transheterozygotes were able to develop apparently
409 normally to the third instar larval stage, and to undergo pupariation. Most lethality occurred at this
410 transition, with obvious defects in air bubble migration and pupal shape. The phenotype was not
411 fully penetrant, and some Nxt1 trans-heterozygote pupae had normal morphology; 20% of
412 transheterozygote third instar pupae survived through to adulthood.

413 The defects in pupal morphology were caused by muscle degeneration during the third instar larval
414 stage. Second instar larvae had normal muscles pattern, morphology and mobility. This indicates
415 that the establishment of the larval musculature, which occurs during embryonic development, is
416 not affected by the reduction in *Nxt1* in the hypomorphic allele.

417 Muscles are composed of tandem arrays of sarcomeres containing thick and thin filaments,
418 arranged in myofibrils. When a muscle twitches, the filaments slide past each other in response to
419 calcium release from the sarcoplasmic reticulum (SR) resulting in force generation. Our
420 examination of the muscle integrity in transheterozygote larvae revealed a variety of defects
421 including muscle atrophy (thinning) and loss of integrity (tearing and splitting). Frequently, we saw
422 loss of filamentous actin in the middle of the muscle while the ends had f-actin; very occasionally
423 we saw balls of muscles associated with loss of attachment or catastrophic failure of muscle
424 integrity and muscle severing. Even when the muscle shape was unaffected, we found a loss of
425 normal internal architecture with disruption of the sarcomeric arrays. Often the muscle was
426 present, but there was filamentous actin staining only towards the ends of the muscle and the
427 central region lacked the sarcomeric structure. It is likely that the reduction in larval mobility, the
428 axial ratio defect, the failure of spiracle eversion and the failure of air bubble movement are all a
429 direct result of the degeneration of muscles in the mutant larvae. All these processes require
430 efficient and coordinated muscle contractions, which are compromised by lack of Nxt1. The curved
431 shape of many mutant pupae is likely to be due to the variability in extent of muscle degeneration:

432 if an individual has more damage on one side than the other, particularly of the longitudinal
433 muscles, there will be unequal contraction as the prepupa forms and one side of the body will
434 shorten more.

435 During the larval phase, the muscles undergo a ~50-fold increase in fibre size. This dramatic
436 growth occurs without addition of new cells, as the number of nuclei in the muscle syncytium
437 remains constant [3]. Increased DNA content is achieved via endoreduplication, and increased
438 muscle volume is driven by cell growth associated with new myofibril and sarcomere assembly [3].
439 The majority of this growth occurs during the third instar larval stage, and depends on nutrient
440 supply and sensing of this via the Insulin/Akt/Tor pathway [32]. Deficits in muscle growth, for
441 example caused by reducing endoreduplication through over expression of cyclinE in muscle, have
442 non-autonomous effects on the growth of the whole larva [32]. We did not detect any difference in
443 the overall size of the third instar mutant larvae, indicating that the defects are not due to defects in
444 nutrient supply or sensing. When *Nxt1* hypomorphic larvae are starved from the late 2$^{nd}$ or early 3$^{rd}$
445 instar larval stage they remain alive and continue to move, but growth is blocked. This treatment
446 was sufficient to rescue the muscle degeneration that typically occurs during the 3$^{rd}$ instar phase.
447 This indicates that the primary cause of the degeneration is defective (re)-organisation during
448 muscle growth, rather than damage caused by use of the muscles, although we cannot rule out
449 that the higher forces required for third instar larval movement are not also implicated.

450

451 **Muscle degeneration can be rescued by increasing *abba***

452 We were surprised that a hypomorphic allele of a pleiotropic factor such as Nxt1 had such a
453 specific phenotype of muscle degeneration. We reasoned that, while it is likely to be important for
454 the normal expression of many genes, reduction in just one or a few crucial genes could underpin
455 the muscle defects. Our initial RNA-seq of whole larvae was a mixed sex population, and
456 unfortunately the majority of genes differentially expressed between samples were those with
457 testes-specific or testis-enriched expression. This is consistent with our previous findings that *Nxt1*
458 is critical for expression of genes regulated by tMAC in testes [19], but meant that the signal from
459 relatively mild expression changes from somatic tissues was less apparent. Nevertheless, one
460 gene, *abba*, with a known role in muscles stood out as being mildly down-regulated in stationary
461 larvae. The phenotype of *abba* mutants is strikingly similar to that we describe for *Nxt1*
462 hypomorphs, particularly with thinner muscles, long thin pupae and defects in both spiracle
463 eversion and air bubble migration [28, 29]. Abba is a TRIM/RBCC protein involved in maintaining
464 the integrity of sarcomeric cytoarchitecture [28, 29], and is the *Drosophila melanogaster*
465 homologue of human *Trim32*, defects in which cause limb girdle muscular dystrophy 2H [15].
466 Trim32 is localised to the costamere, which overlies the Z-disk and ensures attachment of the
467 sarcomere to the overlying extracellular matrix via the dystrophin glycoprotein complex.

468 The phenotypes of defective sarcomere structure, fraying and muscular atrophy are all consistent
469 with reduction in *abba* (costamere) function. The growth of muscles involves the generation of new
470 sarcomeric units, each requiring a new costamere and thus new Abba production and
471 incorporation. The gradual decline in muscle integrity seen during growth may be attributable to
472 reduction in Abba protein levels meaning that the stability of newly formed sarcomeres is reduced.
473 Indeed, in mouse, the expression of Trim32 is upregulated in muscles that are remodelling [33].
474 Consistent with this model, increasing expression of *abba* using a cDNA construct driven with the
475 Gal4/UAS system is sufficient to rescue the muscle defects seen in *Nxt1* mutants. Starvation from
476 late second or early third instar larval stage is also sufficient to rescue the muscle defect. In this
477 case, there is no muscle growth, so no new sarcomeric units need to be added, the existing
478 structures are maintained, and thus there is no muscle degeneration. The rescue by a cDNA also
479 indicates that it is the reduction in *abba* mRNA, rather than a reduction in *abba* circRNA that is
480 important for the muscle phenotype, as the cDNA construct cannot generate the circRNA.

481 RNAi constructs to disrupt Nxt1 function in muscles caused degeneration, again without pattern
482 defects even in second instar larvae, indicating that the precise level of Nxt1 function is critical.
483 Very high level, muscle specific, RNAi construct expression, driven from embryonic stages,
484 presumably reduces the level of active Nxt1 in muscles in embryos and early larval stages even
485 beyond that found in the hypomorphic allele combination. In this situation, there would be reduced
486 Abba both during embryonic muscle formation and at the early growth stages, and this would
487 impact on the muscle integrity even before the extensive third instar larval growth period. Driving
488 *Nxt1* RNAi ubiquitously but at a lower level, phenocopies the *Nxt1* transheterozygote situation, with
489 viability to third instar stage and muscle degeneration in these animals. Driving RNAi targeted
490 against other RNA export pathway factors ubiquitously, with arm-gal4, also phenocopies the Nxt1
491 transheterozygote situation. Importantly, these experiments, coupled with the partial rescue of the
492 muscle defects by expression of Nxt1, confirm that the phenotype is caused by reduction in Nxt1
493 function rather than by a different gene or by a neomorphic effect of the point mutation in $Nxt1^{Z2-}$
494 $^{0488}$. Additionally, these experiments confirm that the role of Nxt1 in muscle maintenance is due to
495 its function in the RNA export pathway, rather than this being a moonlighting function for the
496 protein.

497

498

499 **_Nxt1_ is particularly important for expression of mRNAs and circRNAs from genes with**
500 **long introns**

501 Transcripts with many and large introns are more sensitive to the loss of Nxt1, which is consistent
502 genes with long introns being sensitive to the loss of the EJC [34]. In direct contrast, genes without
503 introns were particularly sensitive to loss of *Nxt1* in testes [19]. RNA-seq data from larval
504 carcasses, which is highly enriched for larval muscles, allowed us to specifically examine the role

505 of Nxt1 in transcript expression in a somatic tissue in which we have shown its function is critical.
506 This revealed a significant relationship between gene expression in *Nxt1* mutants and intron length
507 for both down and up regulated genes. For down-regulated genes, the more dramatic the down-
508 regulation, the longer the total intron length. Similarly, for up regulated genes, the more up
509 regulated the gene, the shorter the total intron length. No strong changes in EJC component
510 transcripts were found in either whole larvae and larval carcasses. Therefore, it is unlikely that
511 defects in EJC component expression levels are implicated in the phenotype. However clearly the
512 ratio between EJC, Nxf1 and Nxt1 will be affected when the level of active Nxt1 is reduced. During
513 primary transcript processing, the spliceosome removes the intron and then the EJC is recruited to
514 the mRNA [25]. The EJC recruits the THO complex, which also recruits UAP56 and REF to form
515 the TREX complex [35]. UAP56 is displaced by the Nxt1-Nxf1 dimer, binding to REF, then REF is
516 removed from the mRNP and Nxt1-Nxf1 binds directly to the mRNP [36]. This process occurs at
517 every intron, although TREX and Nxt1-Nxf1 can also load onto transcripts in the absence of
518 splicing [37]. Transcripts with many introns have more Nxt1-Nxf1 dimer recruitment. If EJC loading
519 is less efficient on transcripts with long introns, particularly if these are being processed to make
520 circRNAs in addition to mRNAs, then these transcripts could be preferentially sensitive to the Nxt1
521 trans-heterozygotes where the availability of Nxt1 protein is limiting.

522

523 Circular RNAs are a relatively recently described class of RNAs that are produced as alternative
524 products from the same primary transcripts as mRNAs. Global analysis of circRNA abundance
525 reveals that many genes can encode circRNAs, but the propensity for a gene to produce a circular
526 transcript is related to the length of the introns, particularly those that flank the back-spliced
527 exon(s) [10]. Our RNA-seq analysis suggests that the mature mRNAs from genes that also
528 produce circRNAs is reduced in Nxt1 mutants. Additionally, we found that the circRNAs
529 themselves are reduced in the mutants. Mutation of exon junction complex components has also
530 been shown to have a preferential effect on mRNA production from genes with long introns [26]. At
531 least some genes down-regulated in the EJC knock down have been shown to have aberrant
532 splicing patterns in the absence of EJC [26]. In contrast, we found few defects in alternative
533 splicing in *Nxt1* mutants. However, it is also interesting to note that 249/315 genes down-regulated
534 after knock down of the EJC were also on the list of genes that produce at least one circRNA, and
535 99 are on the higher confidence list of 10 or more circRNAs [13, 26]. The RNA export pathway has
536 already been shown to be linked to 3' end processing and poly adenylation. TREX subunit THOC5
537 is recruited to target transcript 3'UTRs by poly adenylation specific factor 100 [38]. Ref association
538 with RNAs is promoted by the 5' cap, by the EJC, and, crucially, also in the 3' UTR by nuclear
539 polyA binding protein (PABPN1) [39]. In light of this, it is likely that the EJC and the export adapter
540 Nxt1 (and other factors in the RNA export pathway) are particularly important in processing of
541 transcripts that are alternatively spliced to produce mRNA and circular RNA outputs. We found that
542 pre-mRNA levels of these target genes are not reduced in the mutants, while mature, poly

543 adenlyated mRNAs are, suggesting that the EJC and export factors are acting to ensure
544 stabilisation of the transcripts until completion of 3' end processing.

545

546 RNA regulation, and particularly RNA splicing has been linked to muscular degenerative diseases
547 [17]. Sequestration of the splicing regulator MBNL1 by RNA containing expanded CUG or CCUG
548 repeats reduces functional MBNL and results in aberant splicing of downstream targets in DM
549 patients [16]. The *Drosophila* orthologue of MBNL1, *mbl*, produces an abundant circRNA similarly
550 one of the many MBNL1 splice variants in humans is a circRNA [11]. *mbl* is expressed in both
551 muscles and the nervous system, and is one of the many circRNA-producing genes whose mRNA
552 is reduced (approximately 10x) in *Nxt1* mutant larvae. The production of the *mbl* circRNA is
553 regulated by Mbl protein itself, in an autoregulatory feedback loop. In vertebrates, it appears that
554 MBNL1 does not regulate production of its own circRNA in neuronal cells, but the effect in muscle
555 has not been determined [18, 40]. Our discovery that defects in an RNA export factor, *Nxt1*, can
556 generate a muscular dystrophy phenotype and is associated with differential expression of specific
557 mRNAs and circRNAs in *Drosophila melanogaster* suggests that investigation of the RNA export
558 pathway, and circRNAs, in context of the disease is warranted.

559

560 **Materials and Methods**

561 ***Drosophila* culture, strains and genetics.**

562 Flies were maintained in standard cornmeal, yeast, dextrose, agar medium, at 25°C unless
563 otherwise stated. For selection of staged larvae, 0.05% bromophenol blue was added to the food.
564 Wandering larvae have blue guts, whereas stationary larvae have no blue or very light blue guts.
565 White prepupae were selected by watching larvae, and harvesting them within an hour of
566 pupariation. $w^{1118}$ was used as a control. *yw ; Nxt1*$^{z2\text{-}0488}$ */ CyO Actin-GFP* and *yw ; Nxt1* $^{DG05102}$ /
567 *CyO Actin-GFP* were crossed to generate *Nxt1*$^{z2\text{-}0488}$ */ Nxt1* $^{DG05102}$ transheterozygotes for analyses
568 [19]. The *Nxt1* mutant larvae were selected by the absence of GFP.

569 VDRC RNAi lines KK107745 (*Nxt1*), P{GD17336}v52631 (*Nxt1*) KK102231 (*thoc5*), KK100882
570 (*Nxf1*) and KK109076 (*Ref1*), were used to analyse muscle integrity in the third instar larvae [41].
571 UAS-eGFP-Nxt1 was described in [19].

572 w;UAS-*abba*$^{fl}$, kindly provided by Hanh T. Nguyen, uses the EST GH06739 (GenBank accession
573 number AY121620) as template to amplify and clone the entire *abba* coding or defined regions of
574 *abba* into the pUAST vector [28]. The 3' end of the construct encodes an HA tag. UAS-stock is in
575 heterozygous condition. Mef2-Gal4 [42] was kindly provided by Michael Taylor (Cardiff University);
576 Arm-Gal4 and UAS-dicer were from Bloomington stock centre.

577

578 **RNA extraction, cDNA synthesis and Quantitative PCR**

579 Total RNA was extracted using Trizol (ThermoFisher Scientific) and then further cleaned up with
580 the RNeasy Mini Kit (Qiagen) according to manufacturer's protocol. The DNaseI step was
581 included. RNA was quantified with a nanodrop ND-1000 (ThermoFisher Scientific) and stored at -
582 80$^{o}$C. For larval carcass RNA sequencing, 30 carcasses were used per replicate in triplicates. For
583 qRT-PCR, either a single carcass or a mix of up to 10 carcasses were used as detailed in the
584 results. cDNA was generated using 100ng total RNA and oligo dT primers with the Superscript III
585 kit (Invitrogen). The cDNA reaction was diluted to 60 or 120µl with $dH_2O$, and 1µl of this cDNA was
586 further diluted with 7µl $dH_2O$ to use as a template in the qRT-PCR reactions. 10µl PowerSybr
587 reagent (ABI) with 1µl of a 10µM solution of each target-specific forward and reverse primers
588 (primer sequences on request) were added for a total reaction of 20µl. The qRT-PCR was
589 performed on a Chromo4 instrument (MJR) using the Opticon Monitor 3 software. *Rp49* was used
590 as a control gene for normalization, fold changes were determined by ΔΔCT. All reactions were
591 performed in triplicate.

592

593 **Scanning Electron Microscopy**

594 Young pupae (<4h) were picked, cleaned with water, and air dried overnight. Up to 6 pupae were
595 put on an aluminium backing plate of a SC500 sputter target. A BIO-RAD SC500 sputter coater
596 was used to coat the non-conducting pupae with ~20nm thick layer of Au90Pd10 according to
597 manufacturer's protocol (Quorum Technologies). After coating, pins were put in a FEI-XL30 Field
598 Emission Gun Environmental Scanning Electron Microscope. For imaging, a 30 µm diameter final
599 aperture with a beam current <1nA was used to take pictures from each pupa at the
600 posterior/anterior end and the middle section.

601

602 **Magnetic Chamber Dissection for larval muscle staining**

603 For larval dissections, a magnetic chamber was used [43]. A magnetic strip, with a 30 mm
604 diameter hole in the middle, was glued on a 76 mm x 51 mm slide with 10 mm of the strip sticking
605 out at all sides. Each magnetic chamber uses 2 centre and 4 corner pins. For constructing all pins,
606 see Figure 1 in [43]. All pins were glued to a vintage metal index tab. A larva is put in the middle of
607 the hole with a drop of low $Ca^{2+}$ saline, HL-3 [44]. Larva are put ventral side and two centre pins
608 are used to prevent the larva from moving by pinning at the most anterior and posterior side.
609 Vannas Spring Scissors – 3mm blades (RS-5618; FineScience) were used for cutting. A dorsal
610 incision cut was made at the posterior end with short shallow cuts between the two tracheas until
611 the anterior end was reached.

612

613 **Phalloidin staining of larval muscles**

614 The larva was cleaned on the magnetic chamber by removing all internal organs carefully. All $Ca^{2+}$
615 saline, HL-3 solution was removed with a P-100 pipette and fresh drops were added two more
616 times while cleaning the larval carcass. The larval carcass was fixated by adding fresh 4%
617 paraformaldehyde in PBS for 2 minutes. All the pins were removed from the larval carcass and the
618 sample was transferred to a glass well with 100μl 4% paraformaldehyde for another hour. The
619 fixative was removed, and the larval carcass was washed twice with 100μl PBS-T (0.1% Triton X-
620 100) for 5 minutes each. Two drops of Alexa Fluor™ 488 Phalloidin (ThermoFisher) was added to
621 1ml of PBS-T. 100μl Alexa Fluor™ 488 Phalloidin mix was added to the well to stain F-actin in
622 larval muscles for 1 hour. Alternatively, FITC phalloidin was used at a final concentration of 1 μg/ml
623 in PBS-T. Phalloidin solution was removed and the larval carcass was washed with PBS-T two
624 times for 5 minutes each. The larva carcass was put on a microscope slide and mounted in 85%
625 glycerol + 2.5% n-propyl gallate. Images were made on an Olympus BX 50 (Olympus) microscope
626 and Hamamatsu ORCA-05G digital camera. For a close-up of the larval muscle sarcomeres
627 pattern, images were taken with a Leica DM6000B upright microscope with HC PL Fluotar
628 20x/0.50 and HCX PL APO 40x/1.25 oil objectives.

629

630 **Criteria for scoring muscle defects in larvae**

631 The integrity of larva muscles was calculated as a percentage from a total of 8 hemisegments. The
632 hemisegments A2-A5 were in the abdominal area and were not damaged by any of the pins. Each
633 hemisegment contained 30 different muscles, so a total of 240 muscles were inspected. The
634 integrity of a muscle is compromised if the muscle is damaged in any way, such as being torn, thin,
635 loss of sarcomeric structure or missing. The muscle damage percentage is the total number of
636 damaged muscles divided by 240 and multiplied by 100.

637

638 **Starvation of larvae**

639 Larvae were fed up to 70, 71, 72 and 73 hours after egg laying (AEL) before removal from the
640 food. The larvae were transferred to a petri dish with a moist filter paper in it to prevent desiccation.
641 Larvae in the petri dish were checked at regular intervals to ensure the filter paper was moist and
642 keep track of the progress of the metamorphosis. Larvae deprived of food 70 hours AEL that
643 survived for four days were analysed for muscle integrity.

644

645 **Mobility Assay**

646 First, second and third instar larvae were used for mobility analysis. Larvae (up to 10) were put in
647 the middle of a 1% agar dish with 1% paraffin oil on one side and an odour (1% 2-propanol) on the

648 other side. Larvae were filmed with a Samsung SDN-550 camera using the micro manager 1.4
649 program for 200 frames, with 1 frame per second (fps) in the dark under red light. Movies were
650 analysed with MtrackJ [45] via Fiji. Larvae were tracked per 20 frames ($1^{st}$ instar) or 10 frames ($2^{nd}$
651 and $3^{rd}$ instars) for at least 100 seconds ($1^{st}$ instar) or 50 seconds ($2^{nd}$ and $3^{rd}$ instar) while larvae
652 were continuously crawling on the plate. Mean speed is calculated in mm/sec.

653

654 **Viability Assay**

655 Third instar larvae were taken from the standard vial and put in a new vial with a low quantity of
656 fresh food for the viability assay. After 5 days of incubation at $25^{o}C$ vials were taken out and pupa
657 lethality was backtracked by looking at 6 different points: 1) larvae that did not pupate (0h APF), 2)
658 no visible development in pupae (24h APF), 3) head eversion and development of the eye (48h
659 APF), 4) bristles on dorsal thorax (72h APF), 5) complete fly development in pupa (72h APF) and
660 6) emerging adults.

661

662 **Whole larvae mRNA sequencing and analysis**

663 Eighteen libraries were prepared from total RNA of $w^{1118}$ and Nxt1 trans-heterozygotes genotypes.
664 Each genotype had samples of three different stages (wandering larvae, stationary larvae and
665 white prepupae) in triplicates. RNA extraction was performed using Trizol (ThermoFisher Scientific)
666 followed by the RNeasy Mini Kit (Qiagen). The samples were sent to the University of Exeter to
667 perform the library preparation (ScriptSeq RNA-Seq Library Preparation Kit (Illumina)) and
668 sequencing. All samples were 100bp paired-end sequenced on an Illumina HiSeq 2500 using
669 standard mode.

670 Each sample was prepared in triplicate, and a sequence depth between 6.4M – 11.1M was
671 achieved with sequencing all libraries. The data was analysed with the Tuxedo suite [46] via
672 GenePattern browser [47]. The lists of genes and their Fragments per Kilobase of Exon per Million
673 Mapped Fragments (FPKM) values were compared and statistically tested between the genotypes
674 with Cuffdiff and were imported to excel and divided into more than 2-fold down regulated, more
675 than 2-fold up regulated and non-differentially expressed lists. The differentially expressed genes
676 that were assigned statistically significant had a p-value of $<0.05$. For analysis of ecdysone-
677 responsive genes we looked for differential expression between mutant and control, minimum of 2-
678 fold up or down regulated and a minimum FPKM value of 10 in at least one condition

679

680 **Larval carcass mRNA sequencing**

681 Six libraries were prepared from total RNA of $w^{1118}$ and Nxt1 trans-heterozygotes genotypes.
682 Stationary larvae from each genotype were taken and samples were generated in triplicates. RNA

683 extraction was performed using a combination of Trizol (ThermoFisher Scientific) and the RNeasy
684 Mini Kit (Qiagen). Libraries were generated using the TruSeq Stranded mRNA Library Prep
685 (Illumina) according to manufacturer's protocol. This library preparation method includes an oligo
686 dT selection to sequence only mature, polyadenylated mRNAs. Samples were sequenced using
687 2x75bp paired-end with the NextSeq 500/550 Mid Output v2 kit (150 cycles; Cat. No. FC-404-
688 2001) on an Illumina NextSeq500 Sequencer (Illumina). Sequencing was performed by the
689 Genome Research Hub at Cardiff University, School of Biosciences

690 Each library achieved a read depth between 21M to 32M reads and the data was analysed through
691 the Tuxedo suite [46]. The list of genes with FPKM values provided by Cuffdiff was used to
692 separate the lists in more than 1.5-, 2-, 4- and 16-fold down regulated, more than 1.5-, 2-, 4- and
693 16-fold up regulated and non-differentially expressed. The differentially expressed genes that were
694 assigned statistically significant had a p-value of <0.05. For graphical display using Excel on log
695 axes, 0.001 was added to all FPKM values.

696

697 **Larval carcass total RNA and circRNA sequencing**

698 For total RNA and circRNA sequencing from larval carcass, a total of 30 larval muscle preparations
699 were used for each replicate. Stationary stage third instar larvae were dissected in PBS using the
700 magnetic chamber before being washed twice in PBS, and then transferred directly into an
701 Eppendorf containing 100μl lysis buffer. Batches of 5-7 larval carcasses were pooled in each
702 Eppendorf before being transferred to -20℃ until all sample collection was complete. No more than
703 1hr elapsed between dissection and lysis. *yw; Nxt1*$^{z2-0488}$ / *Nxt1*$^{DG0510}$ larvae were used for mutant
704 analysis, with *w*$^{1118}$ controls for comparison.

705

706 RNA was extracted using the RNAeasy Mini Kit (Qiagen) according to manufacturer's
707 recommendation with on-column DNAseI digestion. RNA quality was checked on a High Sensitivity
708 tape on the TapeStation 2200 (Agilent Technologies) and quantity was checked by Qubit. 1 μg of
709 RNA was treated with 20 units of RNAseR (Epicentre) in a 25μl reaction at 37°C for 30 minutes.
710 Mock samples were treated with the same volume of water. All samples were then cleaned up with
711 2 volumes of RNA Clean XP beads (Agencourt) and eluted with 13 μl of water. 10 μl of mock and
712 RNAseR treated samples were used to make RNA libraries using the TruSeq Stranded total RNA-
713 seq with Ribozero gold LT kit (Illumina) following manufacturers recommendations. Libraries were
714 pooled in equimolar proportions and sequenced on a 2x75bp High-output NextSeq500 cartridge,
715 yielding on average of 40 million reads per sample. All sequencing was performed by the Genome
716 Research Hub at Cardiff University, School of Biosciences.

717

718 **Total RNA-seq Analysis.**

719 Quality control analyses were performed on all samples using FastQC v 0.10
720 (http://www.bioinformatics.babraham.ac.uk/projects/fastqc/). Raw reads were trimmed with
721 trimmomatic v.0.36 [Bolger et al, 2014] (HEADCROP:15 LEADING:3 TRAILING:3
722 SLIDINGWINDOW:4:15 MINLEN:36). Sequence reads were aligned to the *Drosophila*
723 *melanogaster* genome (Dm6.23) using STAR v.2.5.3a [48] with options: --outMultimapperOrder
724 Random --outSAMmultNmax 1. Flybase r6.23 annotations were supplied to index the genome but
725 annotations were not provided for mapping. A second QC analysis was run using Bamtools v.2.4.1
726 [49] and the MarkDuplicate tool from the Picard suite v.2.18.14
727 (https://broadinstitute.github.io/picard/).

728

729 High rates of duplicated and multi-mapping reads were observed in all samples. Upon thorough
730 investigation, we concluded that those were not artificial. Duplication rates were due to a very high
731 abundance of a small number of genes, and was linked to multi-mappers (i.e., multi-mapping reads
732 were also duplicated). Multi-mapping was due to a small rRNA contamination, and highly
733 expressed small RNA (e.g. cuticle gene Cpr49Ac) or RNA with repeated conserved domains (e.g.
734 cuticle genes lcp1 and lcp2). Differential expression analyses were also run with and without
735 deduplication and led to the same conclusions. Multi-mappers were excluded from further analyses
736 but duplicated reads were kept.

737

738 Read counts were generated using Subread package FeatureCounts v. 1.6.2 [50]; reads mapping
739 to one location were assigned to exons (for mRNA) or introns (for pre-mRNA) and reported by
740 gene_id. (metafeature). DESeq2 (Love et al, 2014) was used to normalise reads counts and
741 calculate fpkm values. For visualization in genome browsers (i.e. Integrative Genomic Browser),
742 strand-specific normalised bigwig files were generated with the bamCoverage tool of the
743 deepyools suite v.3.0.1 (--ignoreDuplicates --effectiveGenomeSize 142573017 --normalizeUsing
744 RPKM).

745

746 **CircRNA Identification.**

747 Paired-end reads were merged prior to analysis. CircRNAs were identified using PTESFinder v.1
748 [51] (parameters -s 65 -u) with alignments to the *Drosophila* genome (Dm6.23) and the UCSC
749 Refseq transcriptome. Only those circRNAs that were identified in at least two RNAseR-treated
750 biological replicates were included in further analyses. This is a stringent criterion given the high
751 variability between RNase R-treated replicates and the sequencing depth [52]. 336 circRNA
752 structures were identified in at least two replicates of both WT and *Nxt1* samples and are included
753 in further analyses.

754

755 As a measure of circRNA abundance, we used the number of back-splice per million mapped
756 reads (BPM), defined as: # reads supporting each structure generated by PTESFinder / total #
757 mapped reads (junctions+canonical) *10^6. We averaged the two highest biological replicates. The
758 corresponding two mock (non RNAseR treated) replicates were used to quantify the spliced RNA
759 (but not necessarily poly adenylated) and pre-mRNA of the host transcript. Plots were generated in
760 R with the ggplot2 package.

761

762

763

764

765

766 ## Acknowledgments

767 We gratefully acknowledge all members of the Cardiff University *Drosophila* community, and
768 particularly Sonia Lopez de Quinto, Michael Taylor and Wynand van der Goes van Naters for
769 helpful input on experimental design and data interpretation throughout the project. We thank Nick
770 Kent and Angela Marchbank in the Cardiff University School of Biosciences Genomics Hub for
771 help with the sequencing, we also thank Lorna Harries, Karen Moore and Ryan Ames in Exeter
772 University for guidance with the circRNA sequencing protocol and analysis. *Drosophila* stocks
773 were provided by Michael Taylor (Cardiff University), Hanh T. Nguyen (Friedrich-Alexander
774 University of Erlangen-Nürnberg, Erlangen, Germany), Vienna Drosophila Resource Centre and
775 Bloomington Drosophila Stock Centre. RNA-seq was carried out by Exeter University sequencing
776 service and by the Cardiff University School of Biosciences Genomics Hub.

777

778 **Data availability**

779 RNA-seq datasets for *w1118* and *Nxt1* transheterozygotes larvae are available via GEO: whole
780 larvae before, during and after puparium formation (GSE125781), and late third instar larval
781 carcass samples (mRNA: GSE125776; total RNA and CircRNA: GSE135591).

782

783 ## Figure Legends

784 **Figure 1 Morphological defects in Nxt1 trans-heterozygote pupae.** A) Nxt1 mutant pupae are
785 typically thinner than wild type, are curved, and have uneverted spiracles. B) Axial ratios show
786 Nxt1 mutants are thinner and longer than wild type. C-E) Scanning electron microscopy shows
787 details of anterior and posterior spiracles wild type and Nxt1 mutant pupal cases. Figure in A was
788 taken from [19].

789

790 **Figure 2**

791 **Nxt1 trans-heterozygote 3$^{rd}$ instar larvae have reduced mobility.** A-B) Image of agar plate and
792 larval tracks (analysed via MtrackJ) with control substance on the left and odour on the right. C-E)
793 Mobility analysis of 1$^{st}$, 2$^{nd}$ and 3$^{rd}$ instars of wild type and Nxt1 trans-heterozygotes. F-G) All 1$^{st}$,
794 2$^{nd}$ and 3$^{rd}$ instar data combined for each genotype. Student's t-test *** p value = <0.001. n.s = not
795 significant.

796

797 **Figure 3**

798 **Nxt1 trans-heterozygote 3$^{rd}$ instar larvae show muscle degeneration.** Muscles of larval
799 carcass preparations (WT A and C, Nxt1 mutants B and D-K) imaged with FITC-phalloidin. A)
800 Overview of wild type 3$^{rd}$ instar larva muscles. B) Overview of *Nxt1*$^{DG05102}$/*Nxt1*$^{Z2-0488}$ 3$^{rd}$ instar larva
801 muscles. C) Higher power image of larva hemisegments from (A). D) Hemisegments from
802 *Nxt1*$^{DG05102}$/*Nxt1*$^{Z2-0488}$ with mild muscle degeneration. E) Higher power image of larva
803 hemisegments from (B). F) Lateral Transverse (LT) 1 and 2 crossover (short arrow). F-G) Short
804 LT4 muscle (long arrow). H) Lateral Oblique (LO) 1 fibre split (red arrow). I) J) LO 1 partially
805 degenerated into small bundle of fibres connected to the Segment Border Muscle (SBM). K) Dorsal
806 Oblique (DO) 2 showing strings of fibres (red dotted lines) attached to each end of the muscle.
807 Samples orientated from posterior (left) to anterior (right). A-E) Scale bar = 1 mm. F-K) Scale bar =
808 200 µm.

809

810 **Figure 4**

811 **Sarcomere structure compromised in degenerating muscles.** A) Wild type muscles stained for
812 actin with phalloidin show normal, ribbed lines, thin filaments. B) Nxt1 trans-heterozygotes non-
813 degenerating muscles with normal, ribbed lines, thin filaments. C) Nxt1 trans-heterozygotes
814 degenerating muscles with compromised thin filaments.

815

816 **Figure 5**

817 **Early 2$^{nd}$ instar muscle degeneration with Nxt1 RNAi.** A-A') Wild type 2$^{nd}$ instar larvae carcass
818 preparations, stained with phalloidin, showing normal muscle composition and no damage. B-B')
819 Signs of muscle degeneration with the RNAi 103146 line driven by Mef2-Gal4 visible in early 2$^{nd}$
820 instars with thinner muscles and fiber damage (see insert B'). C-C') Similar degeneration defects
821 shown for the RNAi 52631 line. A-C) Scale bar = 1mm. A'-C') Scale bar = 0.5mm.

822

823 **Figure 6**

824 **Rescue of Nxt1 trans-heterozygote phenotypes.** Nxt1 transheterozygote defects in viability (A),
825 pupal morphology (axial ratios of pupae, B), muscle morphology (C) and 3rd instar motility (D) were
826 partially rescued by over-expression of GFP-Nxt1 in muscles (Mef2-Gal4) or ubiquitously (arm-
827 Gal4).

828

829 **Figure 7**

830 **Nxt1 trans-heterozygote muscles do not degenerate when larval growth is prevented.** A)
831 Nxt1 trans-heterozygote pupae were smaller, but had normal morphology when food was withheld
832 from 70h AEL. Three food-deprived and three normal feeding animals are shown. B) Nxt1 trans-
833 heterozygote 70h AEL were examined for muscle degeneration. Individuals that had not pupated
834 four days after no feeding still had intact muscles (N= 10).

835

836 **Figure 8**

837 **Muscle degeneration caused by RNAi against other RNA export pathway genes.**

838 A, A') Control arm-gal4 driver line late 3rd instar larvae muscles stained with phalloidin shows
839 normal muscle structure. B-E) Muscle degeneration observed after ubiquitous, moderate, induction
840 of RNAi against *Nxt1* (B, B'), *Nxf1* (C, C') , *Ref1* (D, D') and *thoc5* (E, E').

841

842 **Figure 9. Genes with long introns are under-expressed in Nxt1 trans-heterozygotes.**

843 mRNA level (FPKM) showing relative expression in WT and Nxt1 larval carcass samples. A) All
844 genes, coloured to show total intron length. Genes with long introns are typically expressed at
845 lower levels in the mutant than in the wild type sample. B) Genes (red in panel A) whose total
846 intron length is >50kb, C) Genes (green in panel A) whose total intron length is between 5 and 15
847 kb, D) Genes (blue in panel A) whose total intron length is <5 kb.

848

849 **Figure 10**

850 **Q-RT-PCR validation of under-expression of genes with long introns in *Nxt1* trans-**
851 **heterozygote larval carcass.** Genes with an average total intron length of 5700, 7500, 10000 and
852 15000 were examined. Expression of *abba* and *Nxt1* are also shown. CG1307 and CG9330 were
853 used as control genes with low total intron length. All genes examined have expression in the
854 carcass. Rp49 was used for normalization.

855

856 **Figure 11**

857 **Reduced expression of circRNAs but not nascent transcripts in *Nxt1* trans-heterozygotes**

858 Expression of nascent RNAs (A) and spliced mRNA that is not necessarily polyadenylated (B) is
859 similar in total RNA samples from WT and mutant larval carcasses. Genes that produce circRNAs
860 are highlighted in red. C, sequencing only polyadenylated transcripts reveals reduction in the
861 expression of the mature mRNA from these genes. D, circRNAs detected by sequencing after
862 RNAseR digestion are reduced in mutant larval carcass compared to WT. E, normalised alignment
863 of sequence reads from the *abba* genomic region from the total RNA sequencing (w/o RNAseR)
864 and circRNA sequencing (with RNAseR) reveals that production of a circRNA from this gene is
865 reduced in mutant larval carcasses.

866

867 **Figure 12**

868 **Increasing *abba* expression rescues Nxt1 trans-heterozygote muscle degeneration.** A)
869 Genomic structure of the longest *abba* transcript including all known domains, exons are broad
870 boxes, introns are narrow lines. B) Q-RT-PCR analysis of expression of *abba* in 10 individual
871 stationary larvae plus a mix of 30 stationary larvae in Nxt1 trans-heterozygotes, compared to a mix
872 of 10 and 30 stationary wild type larvae, respectively. C) Increasing *abba* with the UAS/Gal4
873 system specifically in muscles rescues muscle degeneration, as revealed by FITC-phalloidin
874 staining. D) Expression of *abba* in 10 individual larvae from the rescue experiment, compared to a
875 mix of 10 stationary wild type larvae. Rp49 was used for normalization.

876

877 **Table 1**

878 **Total intron lengths for genes down and up regulated from larval carcass sequencing.**
879 Genes down regulated have longer total intron length compared to up regulated and non-
880 differentially expressed genes. The total intron length becomes longer with the more highly down
881 regulated genes. Down regulated genes have more introns and their largest intron is significantly
882 longer.

883

884 **Table 2**

885 **Transcript lengths from down and up regulated genes.** Genes that are down regulated also
886 have a longer transcript length compared to up regulated and non-differentially expressed genes.
887 For down regulated genes, the number of transcripts is higher and their shortest/longest transcripts
888 are larger.

889

890 **Supplementary figure 1**

891 **Air bubble movement fails in Nxt1 trans-heterozygote pupae.** Still images of wild type (upper)
892 and Nxt1 trans-heterozygotes (lower) for 15 hours. A) Faint visibility of air bubble in both
893 genotypes. B-D) Air bubble becomes more prominent. E-G) Air bubble is clearly visible halfway
894 along the pupa. I-L) Air bubble expands further. M) Air bubble has disappeared and permitted head
895 eversion for wild type, whereas Nxt1 mutant still show air bubble. N) Larva body in Nxt1 mutant
896 released from cuticle at posterior end and retracts to anterior. O-P) No further changes observed in
897 both genotypes.

898

899 **Supplementary figure 2**

900 **Timing of pupal lethality in Nxt1 trans-heterozygotes.** Pupae were examined at six different
901 time points. Many Nxt1 mutants had defects in head eversion, which becomes visible 48 hours into
902 the pupa phase. Nxt1 hypomorph/+ heterozygotes showed a slight reduction in pupa viability.

903

904 **Supplementary figure 3**

905 R**educed expression of spliced but not nascent *abba* transcripts in *Nxt1* trans-**
906 **heterozygotes.** A) Overview of six different *abba* isoforms, including the four regions used for
907 nascent vs. spliced transcript analysis. B) qRT-PCR of four different regions in *abba* comparing
908 nascent vs. spliced expression. *Rp49* was used for normalization.

909

910 Supplementary table 1

911 **Known ecdysone responsive genes are not under-expressed in *Nxt1* trans-heterozygotes.**
912 Ecdysone responsive genes [21] were examined by looking their differential expression status in
913 whole larval RNA-seq data from cuffdiff (P-value <0.05), a minimum fold change of 2 and a FPKM
914 threshold of at least 10 FPKM in one of the two genotypes.

915

916 Supplementary table 2

917 **Overview of larval muscle genes from whole larval RNA sequencing.** Thirteen larval muscle
918 genes with log2 fold change from RNA sequencing showing majority of genes up regulated with
919 only one down regulated. Red = more than 1.5-fold down regulated. Green = more than 1.5-fold up
920 regulated.

921

922

## References


1. Bate M. The embryonic development of larval muscles in Drosophila. Development (Cambridge, England). 1990;110(3):791-804.
2. Kim JH, Jin P, Duan R, Chen EH. Mechanisms of myoblast fusion during muscle development. Current opinion in genetics & development. 2015;32:162-70. Epub 2015/05/20. doi: 10.1016/j.gde.2015.03.006. PubMed PMID: 25989064; PubMed Central PMCID: PMCPMC4508005.
3. Piccirillo R, Demontis F, Perrimon N, Goldberg AL. Mechanisms of muscle growth and atrophy in mammals and Drosophila. Developmental Dynamics. 2014;243(2):201-15. doi: 10.1002/dvdy.24036.
4. Shatoury HH. The Development of a Pupal Lethal Mutant in Drosophila. Caryologia. 1959;12:1:104-9.
5. Carmody SR, Wente SR. mRNA nuclear export at a glance. J Cell Sci. 2009;122:1933-7.
6. Strasser K, Masuda S, Mason P, Pfannstiel J, Oppizzi M, Rodriguez-Navarro S, et al. TREX is a conserved complex coupling transcription with messenger RNA export. Nature. 2002;417(6886):304-8. Epub 2002/04/30. doi: 10.1038/nature746. PubMed PMID: 11979277.
7. Boehm V, Gehring NH. Exon Junction Complexes: Supervising the Gene Expression Assembly Line. Trends in Genetics. 2016;32(11):724-35. doi: https://doi.org/10.1016/j.tig.2016.09.003.
8. Huang S, Yang B, Chen BJ, Bliim N, Ueberham U, Arendt T, et al. The emerging role of circular RNAs in transcriptome regulation. Genomics. 2017;109(5):401-7. doi: https://doi.org/10.1016/j.ygeno.2017.06.005.
9. Li X, Yang L, Chen L-L. The Biogenesis, Functions, and Challenges of Circular RNAs. Molecular Cell. 2018;71(3):428-42. doi: https://doi.org/10.1016/j.molcel.2018.06.034.
10. Jeck WR, Sorrentino JA, Wang K, Slevin MK, Burd CE, Liu J, et al. Circular RNAs are abundant, conserved, and associated with ALU repeats. RNA (New York, NY). 2013;19(2):141-57.
11. Ashwal-Fluss R, Meyer M, Pamudurti Nagarjuna R, Ivanov A, Bartok O, Hanan M, et al. circRNA Biogenesis Competes with Pre-mRNA Splicing. Molecular Cell. 2014;56(1):55-66. doi: https://doi.org/10.1016/j.molcel.2014.08.019.
12. Zhang Y, Xue W, Li X, Zhang J, Chen S, Zhang J-L, et al. The Biogenesis of Nascent Circular RNAs. Cell Reports. 2016;15(3):611-24. doi: https://doi.org/10.1016/j.celrep.2016.03.058.
13. Westholm Jakub O, Miura P, Olson S, Shenker S, Joseph B, Sanfilippo P, et al. Genome-wide Analysis of Drosophila Circular RNAs Reveals Their Structural and Sequence Properties and Age-Dependent Neural Accumulation. Cell Reports. 2014;9(5):1966-80. doi: https://doi.org/10.1016/j.celrep.2014.10.062.
14. Hoffman EP, Brown RH, Kunkel LM. Dystrophin: The protein product of the duchenne muscular dystrophy locus. Cell. 1987;51(6):919-28. doi: https://doi.org/10.1016/0092-8674(87)90579-4.
15. Frosk P, Weiler T, Nylen E, Sudha T, Greenberg CR, Morgan K, et al. Limb-girdle muscular dystrophy type 2H associated with mutation in TRIM32, a putative E3-ubiquitin-ligase gene. American journal of human genetics. 2002;70(3):663-72. Epub 01/29. doi: 10.1086/339083. PubMed PMID: 11822024.
16. Meola G, Cardani R. Myotonic dystrophies: An update on clinical aspects, genetic, pathology, and molecular pathomechanisms. Biochimica et Biophysica Acta (BBA) - Molecular Basis of Disease. 2015;1852(4):594-606. doi: https://doi.org/10.1016/j.bbadis.2014.05.019.
17. Wheeler TM, Thornton CA. Myotonic dystrophy: RNA-mediated muscle disease. Current Opinion in Neurology. 2007;20(5):572-6. doi: 10.1097/WCO.0b013e3282ef6064. PubMed PMID: 00019052-200710000-00011.

18. Konieczny P, Stepniak-Konieczna E, Sobczak K. MBNL expression in autoregulatory feedback loops. RNA Biology. 2018;15(1):1-8. doi: 10.1080/15476286.2017.1384119.
19. Caporilli S, Yu Y, Jiang J, White-Cooper H. The RNA export factor, Nxt1, is required for tissue specific transcriptional regulation. PLoS genetics. 2013;9(6):e1003526. Epub 2013/06/12. doi: 10.1371/journal.pgen.1003526. PubMed PMID: 23754955; PubMed Central PMCID: PMCPmc3674997.
20. Yamanaka N, Rewitz KF, O'Connor MB. Ecdysone control of developmental transitions: lessons from Drosophila research. Annual review of entomology. 2013;58:497-516. Epub 10/15. doi: 10.1146/annurev-ento-120811-153608. PubMed PMID: 23072462.
21. Fletcher JC, Thummel CS. The Drosophila E74 gene is required for the proper stage- and tissue-specific transcription of ecdysone-regulated genes at the onset of metamorphosis. Development (Cambridge, England). 1995;121(5):1411-21. Epub 1995/05/01. PubMed PMID: 7789271.
22. Wright LG, Chen T, Thummel CS, Guild GM. Molecular characterization of the 71E late puff in Drosophila melanogaster reveals a family of novel genes. J Mol Biol. 1996;255(3):387-400. Epub 1996/01/26. doi: 10.1006/jmbi.1996.0032. PubMed PMID: 8568884.
23. Vaskova M, Bentley AM, Marshall S, Reid P, Thummel CS, Andres AJ. Genetic analysis of the Drosophila 63F early puff. Characterization of mutations in E63-1 and maggie, a putative Tom22. Genetics. 2000;156(1):229-44. Epub 2000/09/09. PubMed PMID: 10978288; PubMed Central PMCID: PMCPMC1461229.
24. Beadle GW, Tatum EL, Clancy CW. Food level in relation to rate of development and eye pigmentation in Drosophilha melanogaster. Bio Bull. 1938;75(3):447-62.
25. Le Hir H, Gatfield D, Izaurralde E, Moore M. The exon-exon junction complex provides a binding platform for factors involved in mRNA export and nonsense-mediated mRNA decay. EMBO J. 2001;20:4987-97.
26. Ashton-Beaucage D, Udell CM, Lavoie H, Baril C, Lefrançois M, Chagnon P, et al. The Exon Junction Complex Controls the Splicing of mapk and Other Long Intron-Containing Transcripts in Drosophila. Cell. 2010;143(2):251-62. doi: https://doi.org/10.1016/j.cell.2010.09.014.
27. Duff MO, Olson S, Wei X, Garrett SC, Osman A, Bolisetty M, et al. Genome-wide identification of zero nucleotide recursive splicing in Drosophila. Nature. 2015;521:376. doi: 10.1038/nature14475 https://www.nature.com/articles/nature14475 - supplementary-information.
28. Domsch K, Ezzeddine N, Nguyen HT. Abba is an essential TRIM/RBCC protein to maintain the integrity of sarcomeric cytoarchitecture. J Cell Sci. 2013;126(Pt 15):3314-23. Epub 2013/06/05. doi: 10.1242/jcs.122366. PubMed PMID: 23729735.
29. LaBeau-DiMenna EM, Clark KA, Bauman KD, Parker DS, Cripps RM, Geisbrecht ER. Thin, a Trim32 ortholog, is essential for myofibril stability and is required for the integrity of the costamere in Drosophila. Proceedings of the National Academy of Sciences of the United States of America. 2012;109(44):17983-8. Epub 10/15. doi: 10.1073/pnas.1208408109. PubMed PMID: 23071324.
30. Herold A, Klymenko T, Izaurralde E. NXF1/p15 heterodimers are essential for mRNA nuclear export in Drosophila. RNA. 2001;7:1768-80.
31. Wiegand HL, Coburn GA, Zeng Y, Kang Y, Bogerd HP, Cullen BR. Formation of Tap/NXT1 heterodimers activates Tap-dependent nuclear mRNA export by enhancing recruitment to nuclear pore complexes. Mol Cell Biol. 2002;22(1):245-56. Epub 2001/12/12. PubMed PMID: 11739738; PubMed Central PMCID: PMCPMC134221.
32. Demontis F, Perrimon N. Integration of Insulin receptor/Foxo signaling and dMyc activity during muscle growth regulates body size in Drosophila. Development (Cambridge, England). 2009;136(6):983-93. Epub 2009/02/13. doi: 10.1242/dev.027466. PubMed PMID: 19211682; PubMed Central PMCID: PMCPMC2727562.
33. Kudryashova E, Kudryashov D, Kramerova I, Spencer MJ. Trim32 is a ubiquitin ligase mutated in limb girdle muscular dystrophy type 2H that binds to skeletal muscle myosin and ubiquitinates actin. J Mol Biol. 2005;354(2):413-24. Epub 2005/10/26. doi: 10.1016/j.jmb.2005.09.068. PubMed PMID: 16243356.
34. Ashton-Beaucage D, Therrien M. The exon junction complex: a splicing factor for long intron containing transcripts? Fly. 2011;5(3):224-33. Epub 2011/04/12. PubMed PMID: 21478676.

029 35. Strässer K, Masuda S, Mason P, Pfannstiel J, Oppizzi M, Rodriguez-Navarro S, et al.
030 TREX is a conserved complex coupling transcription with messenger RNA export. Nature.
031 2002;417:304-8.
032 36. Strasser K, Hurt E. Yra1p, a conserved nuclear RNA-binding protein, interacts directly with
033 Mex67p and is required for mRNA export. EMBO J. 2000;19(3):410-20. Epub 2000/03/18. doi:
034 10.1093/emboj/19.3.410. PubMed PMID: 10722314; PubMed Central PMCID: PMCPMC305578.
035 37. Viphakone N, Sudbery I, Griffith L, Heath CG, Sims D, Wilson SA. Co-transcriptional
036 Loading of RNA Export Factors Shapes the Human Transcriptome. Molecular Cell.
037 2019;75(2):310-23.e8. doi: 10.1016/j.molcel.2019.04.034.
038 38. Tran DDH, Saran S, Williamson AJK, Pierce A, Dittrich-Breiholz O, Wiehlmann L, et al.
039 THOC5 controls 3′end-processing of immediate early genes via interaction with polyadenylation
040 specific factor 100 (CPSF100). Nucleic Acids Research. 2014;42(19):12249-60. doi:
041 10.1093/nar/gku911.
042 39. Shi M, Zhang H, Wu X, He Z, Wang L, Yin S, et al. ALYREF mainly binds to the 5′ and the
043 3′ regions of the mRNA in vivo. Nucleic Acids Research. 2017;45(16):9640-53. doi:
044 10.1093/nar/gkx597.
045 40. Konieczny P, Stepniak-Konieczna E, Taylor K, Sznajder ŁJ, Sobczak K. Autoregulation of
046 MBNL1 function by exon 1 exclusion from MBNL1 transcript. Nucleic Acids Research.
047 2017;45(4):1760-75. doi: 10.1093/nar/gkw1158.
048 41. Dietzl G, Chen D, Schnorrer F, Su K, Barinova Y, Fellner M, et al. A genome-wide
049 transgenic RNAi library for conditional gene inactivation in Drosophila. Nature. 2007;448:151-6.
050 42. Ranganayakulu G, Schulz RA, Olson EN. Wingless Signaling InducesnautilusExpression in
051 the Ventral Mesoderm of theDrosophilaEmbryo. Developmental Biology. 1996;176(1):143-8. doi:
052 https://doi.org/10.1006/dbio.1996.9987.
053 43. Budnik V, Gorczyca M, Prokop A. Selected methods for the anatomical study of drosophila
054 embryonic and larval neuromuscular junctions. Budnik V, Ruiz-Canada C, editors: International
055 Review of Neurobiology; 2006.
056 44. Pesavento PA, Stewart RJ, Goldstein LSB. Characterization of the KLP68D kinesin-like
057 protein in *Drosophila*: possible roles in axonal transport. J Cell Biol. 1994;127(4):1041-8.
058 45. Meijering E, Dzyubachyk O, Smal I. Methods for cell and particle tracking. Methods in
059 enzymology. 2012;504:183-200. Epub 2012/01/24. doi: 10.1016/b978-0-12-391857-4.00009-4.
060 PubMed PMID: 22264535.
061 46. Trapnell C, Roberts A, Goff L, Pertea G, Kim D, Kelley DR, et al. Differential gene and
062 transcript expression analysis of RNA-seq experiments with TopHat and Cufflinks. Nat Protoc.
063 2012;7(3):562-78. Epub 2012/03/03. doi: 10.1038/nprot.2012.016. PubMed PMID: 22383036;
064 PubMed Central PMCID: PMCPMC3334321.
065 47. Reich M, Liefeld T, Gould J, Lerner J, Tamayo P, Mesirov JP. GenePattern 2.0. Nature
066 genetics. 2006;38(5):500-1. Epub 2006/04/28. doi: 10.1038/ng0506-500. PubMed PMID:
067 16642009.
068 48. Dobin A, Davis CA, Schlesinger F, Drenkow J, Zaleski C, Jha S, et al. STAR: ultrafast
069 universal RNA-seq aligner. Bioinformatics (Oxford, England). 2012;29(1):15-21. doi:
070 10.1093/bioinformatics/bts635.
071 49. Barnett DW, Garrison EK, Quinlan AR, Strömberg MP, Marth GT. BamTools: a C++ API
072 and toolkit for analyzing and managing BAM files. Bioinformatics (Oxford, England).
073 2011;27(12):1691-2. doi: 10.1093/bioinformatics/btr174.
074 50. Liao Y, Smyth GK, Shi W. featureCounts: an efficient general purpose program for
075 assigning sequence reads to genomic features. Bioinformatics (Oxford, England). 2014;30(7):923-
076 30. Epub 2013/11/15. doi: 10.1093/bioinformatics/btt656. PubMed PMID: 24227677.
077 51. Izuogu OG, Alhasan AA, Alafghani HM, Santibanez-Koref M, Elliott DJ, Jackson MS.
078 PTESFinder: a computational method to identify post-transcriptional exon shuffling (PTES) events.
079 BMC Bioinformatics. 2016;17(1):31. doi: 10.1186/s12859-016-0881-4.
080 52. Szabo L, Salzman J. Detecting circular RNAs: bioinformatic and experimental challenges.
081 Nature Reviews Genetics. 2016;17:679. doi: 10.1038/nrg.2016.114.

082

# Figure 1

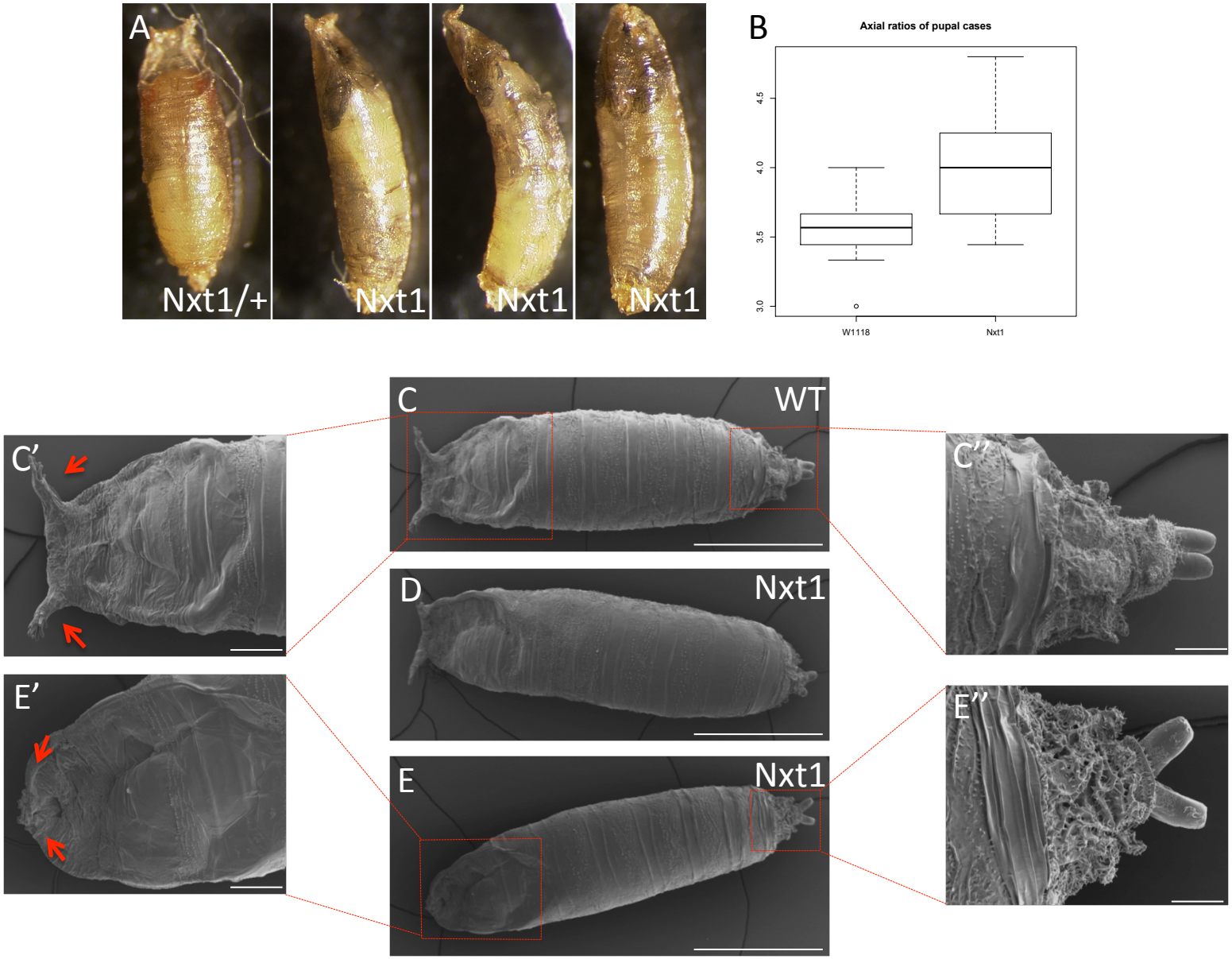
A
Nxt1/+
Nxt1
Nxt1
Nxt1
B
Axial ratios of pupal cases
4.5
4.0
3.5
3.0
W1118
Nxt1
C
WT
C'
C''
D
Nxt1
E'
E
Nxt1
E''

# Figure 2

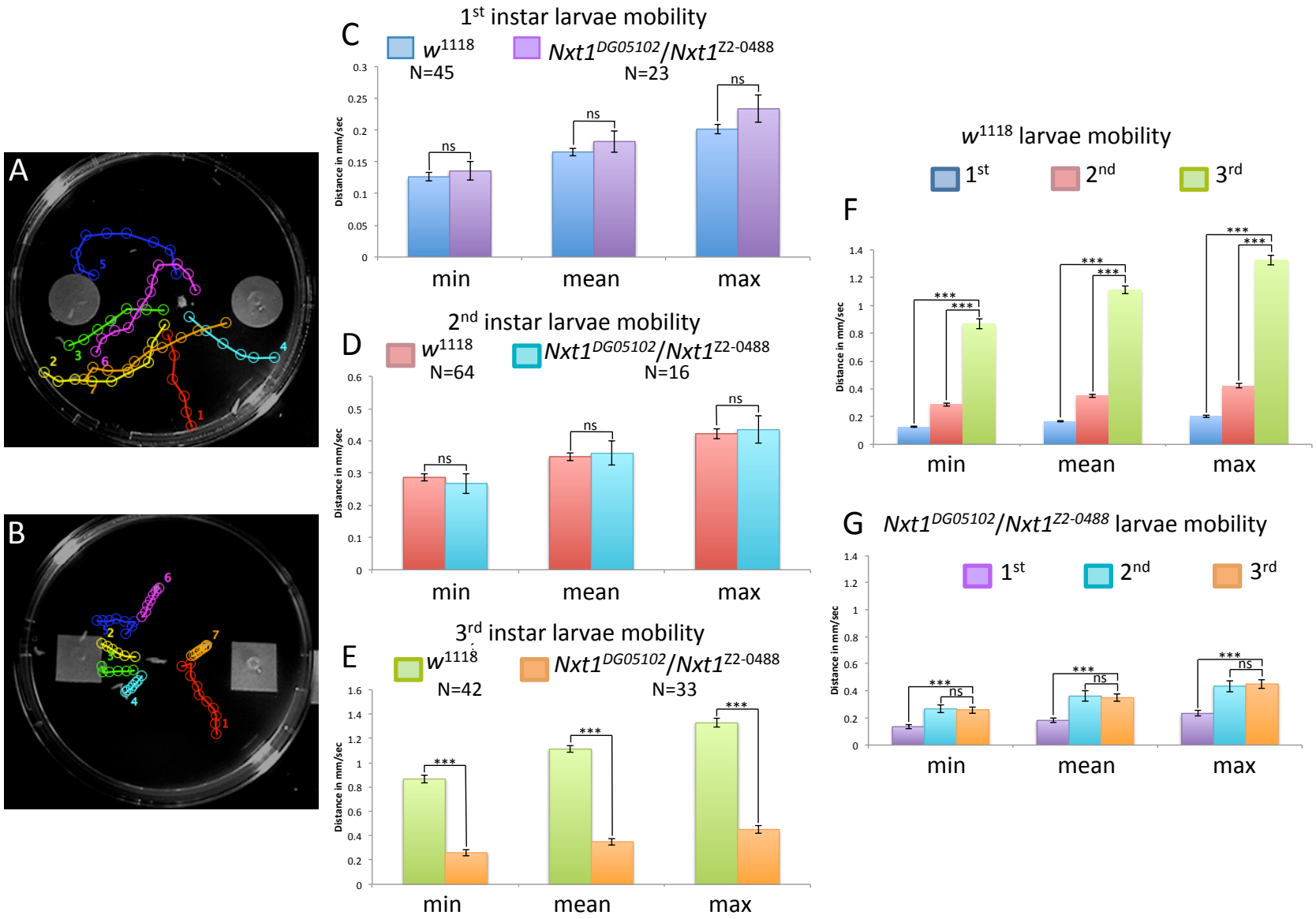
A
B
C
1st instar larvae mobility
w1118
N=45
Nxt1DG05102/Nxt1Z2-0488
N=23
Distance in mm/sec
ns
min
mean
max
D
2nd instar larvae mobility
w1118
N=64
Nxt1DG05102/Nxt1Z2-0488
N=16
E
3rd instar larvae mobility
w1118
N=42
Nxt1DG05102/Nxt1Z2-0488
N=33
***
F
w1118 larvae mobility
1st
2nd
3rd
G
Nxt1DG05102/Nxt1Z2-0488 larvae mobility

# Figure 3

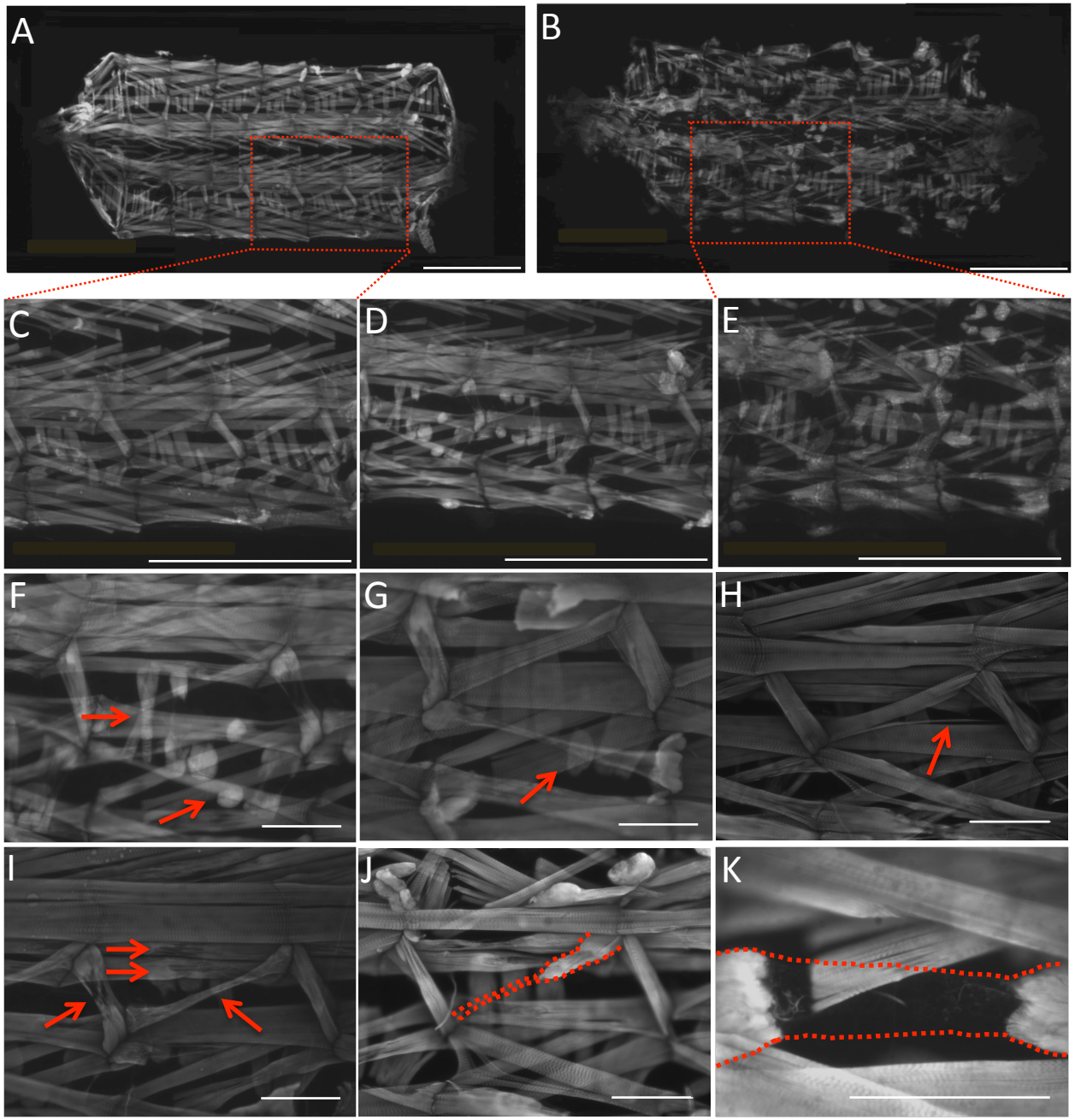

# Figure 4

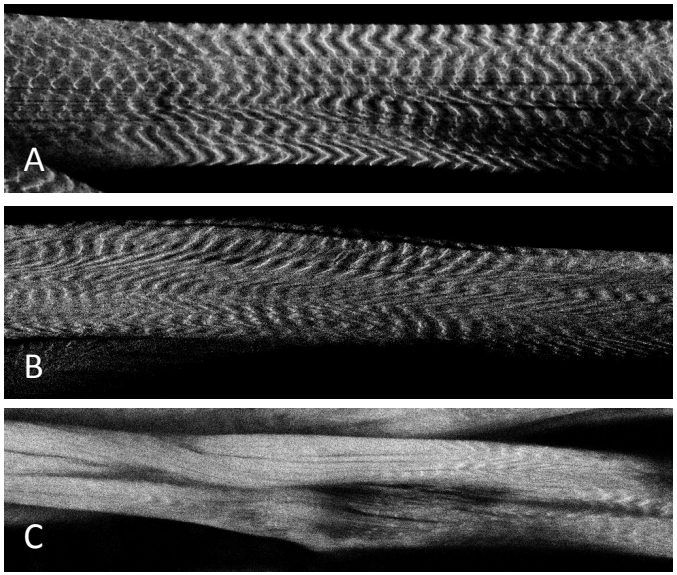

# Figure 5

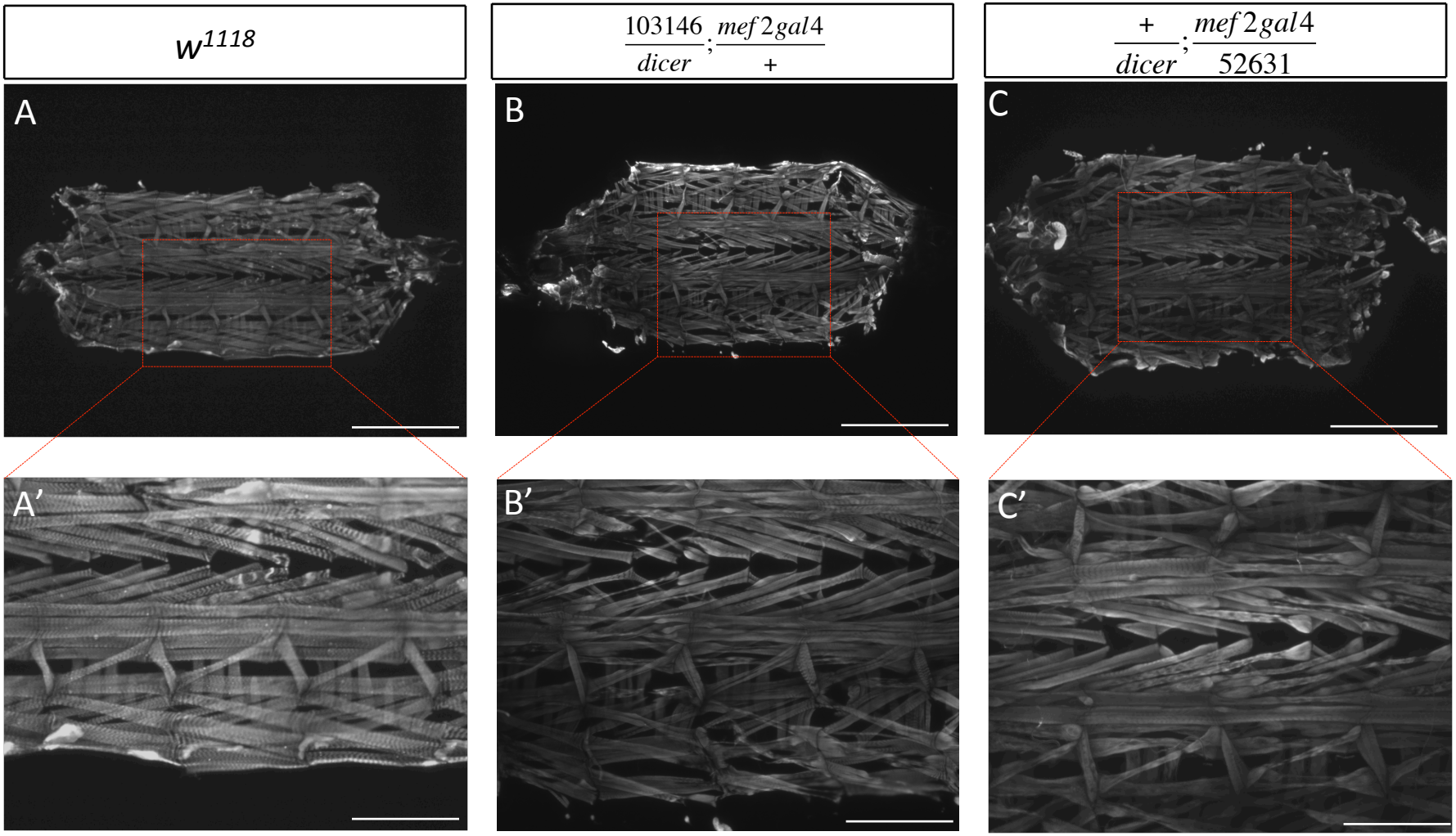
$w^{1118}$
$\frac{103146}{dicer};\frac{mef2gal4}{+}$
$\frac{+}{dicer};\frac{mef2gal4}{52631}$
A
B
C
A'
B'
C'

# Figure 6

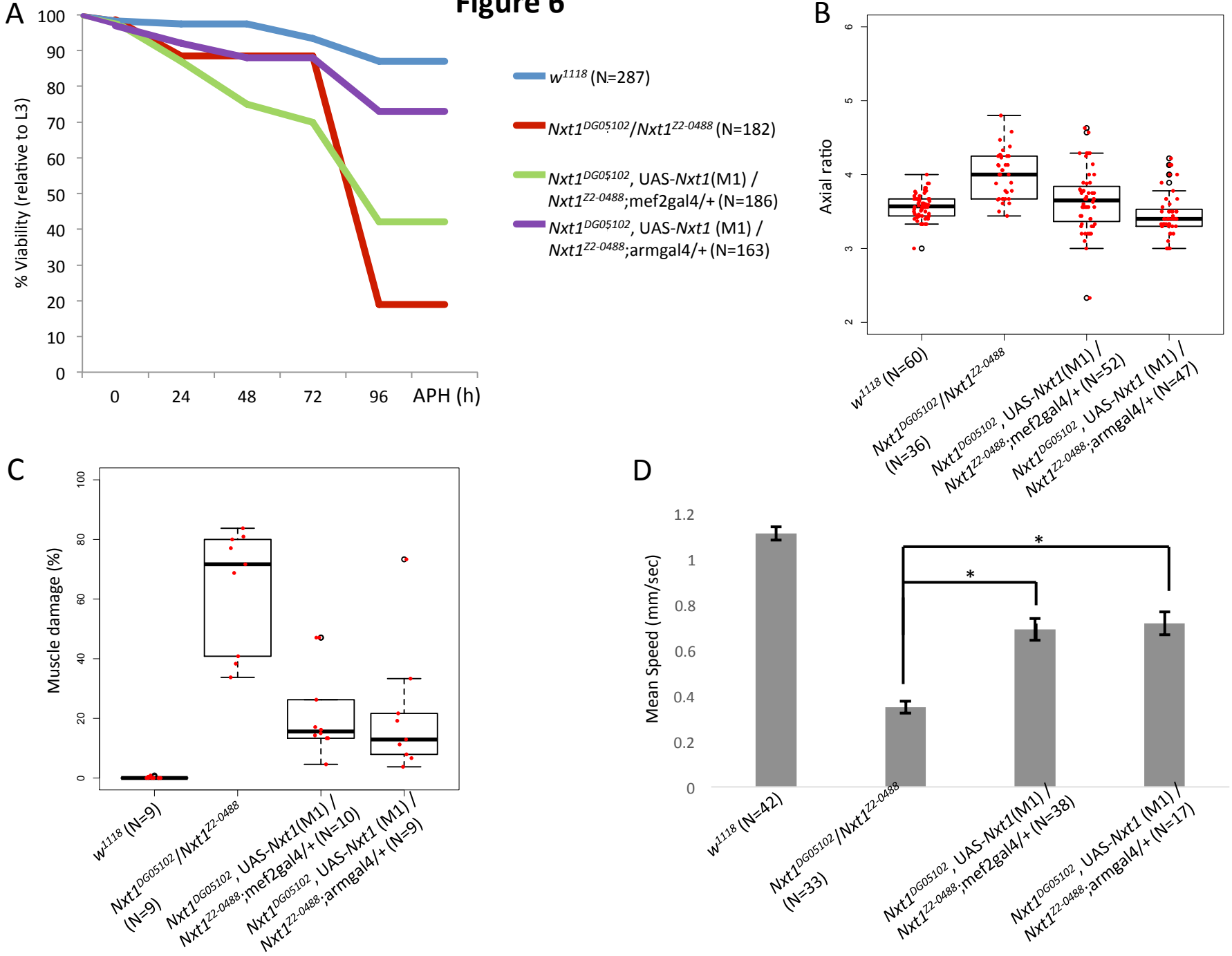
A
% Viability (relative to L3)
100
90
80
70
60
50
40
30
20
10
0
0
24
48
72
96
APH (h)
w1118 (N=287)
Nxt1DG05102/Nxt1Z2-0488 (N=182)
Nxt1DG05102, UAS-Nxt1(M1) / Nxt1Z2-0488;mef2gal4/+ (N=186)
Nxt1DG05102, UAS-Nxt1 (M1) / Nxt1Z2-0488;armgal4/+ (N=163)
B
Axial ratio
w1118 (N=60)
Nxt1DG05102/Nxt1Z2-0488 (N=36)
Nxt1DG05102, UAS-Nxt1(M1) / Nxt1Z2-0488;mef2gal4/+ (N=52)
Nxt1DG05102, UAS-Nxt1 (M1) / Nxt1Z2-0488;armgal4/+ (N=47)
C
Muscle damage (%)
w1118 (N=9)
Nxt1DG05102/Nxt1Z2-0488 (N=9)
Nxt1DG05102, UAS-Nxt1(M1) / Nxt1Z2-0488;mef2gal4/+ (N=10)
Nxt1DG05102, UAS-Nxt1 (M1) / Nxt1Z2-0488;armgal4/+ (N=9)
D
Mean Speed (mm/sec)
1.2
1
0.8
0.6
0.4
0.2
0
*
*
w1118 (N=42)
Nxt1DG05102/Nxt1Z2-0488 (N=33)
Nxt1DG05102, UAS-Nxt1(M1) / Nxt1Z2-0488;mef2gal4/+ (N=38)
Nxt1DG05102, UAS-Nxt1 (M1) / Nxt1Z2-0488;armgal4/+ (N=17)

**Figure. 7**

*Nxt1* trans-heterozygotes

Stopped feeding
70h AEL

Feeding normally

70h AEL

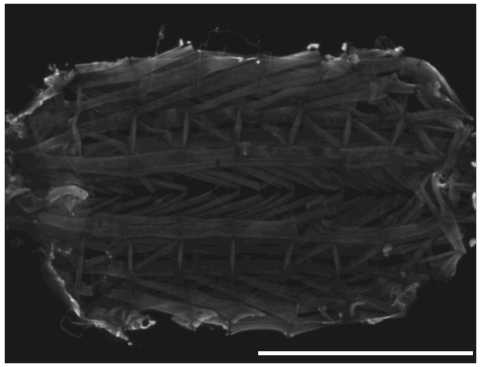

70h AEL +4d

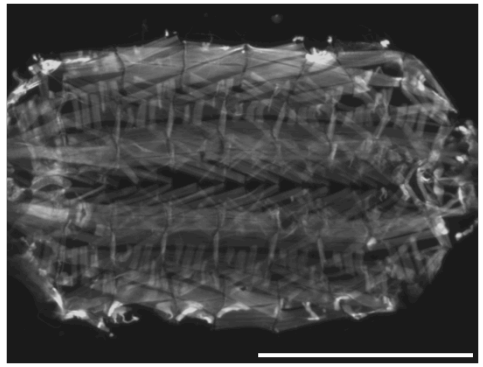

**Figure 8**

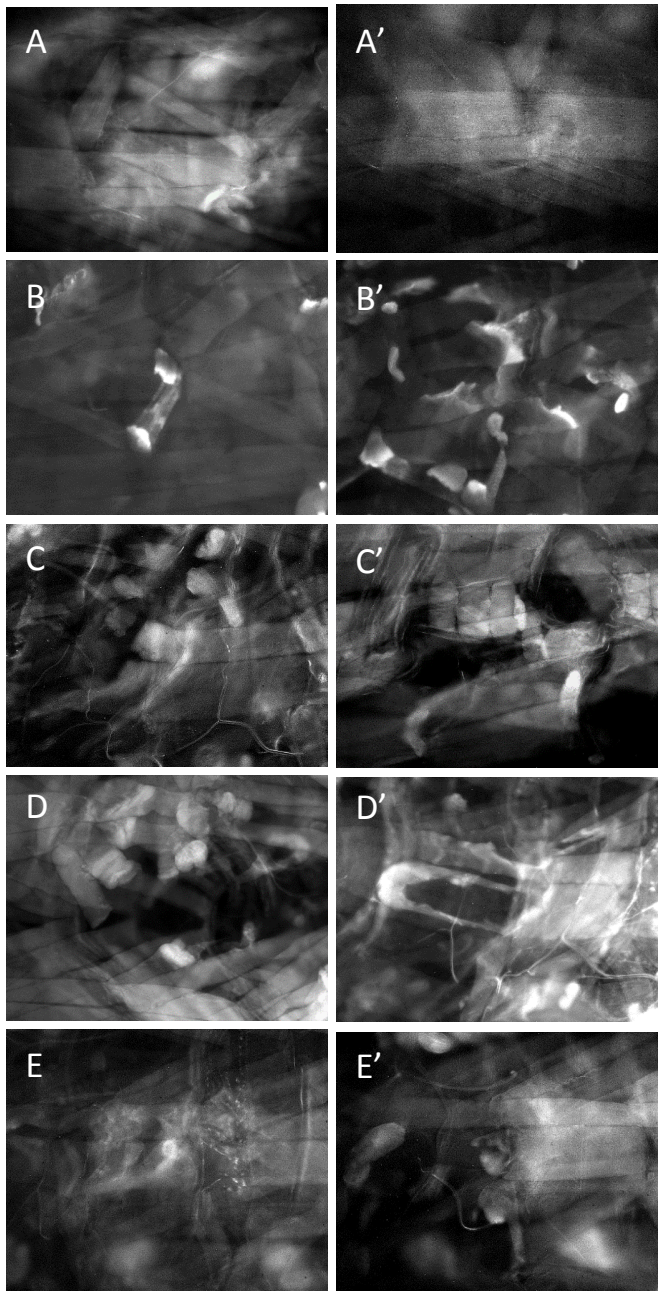

# Figure 9

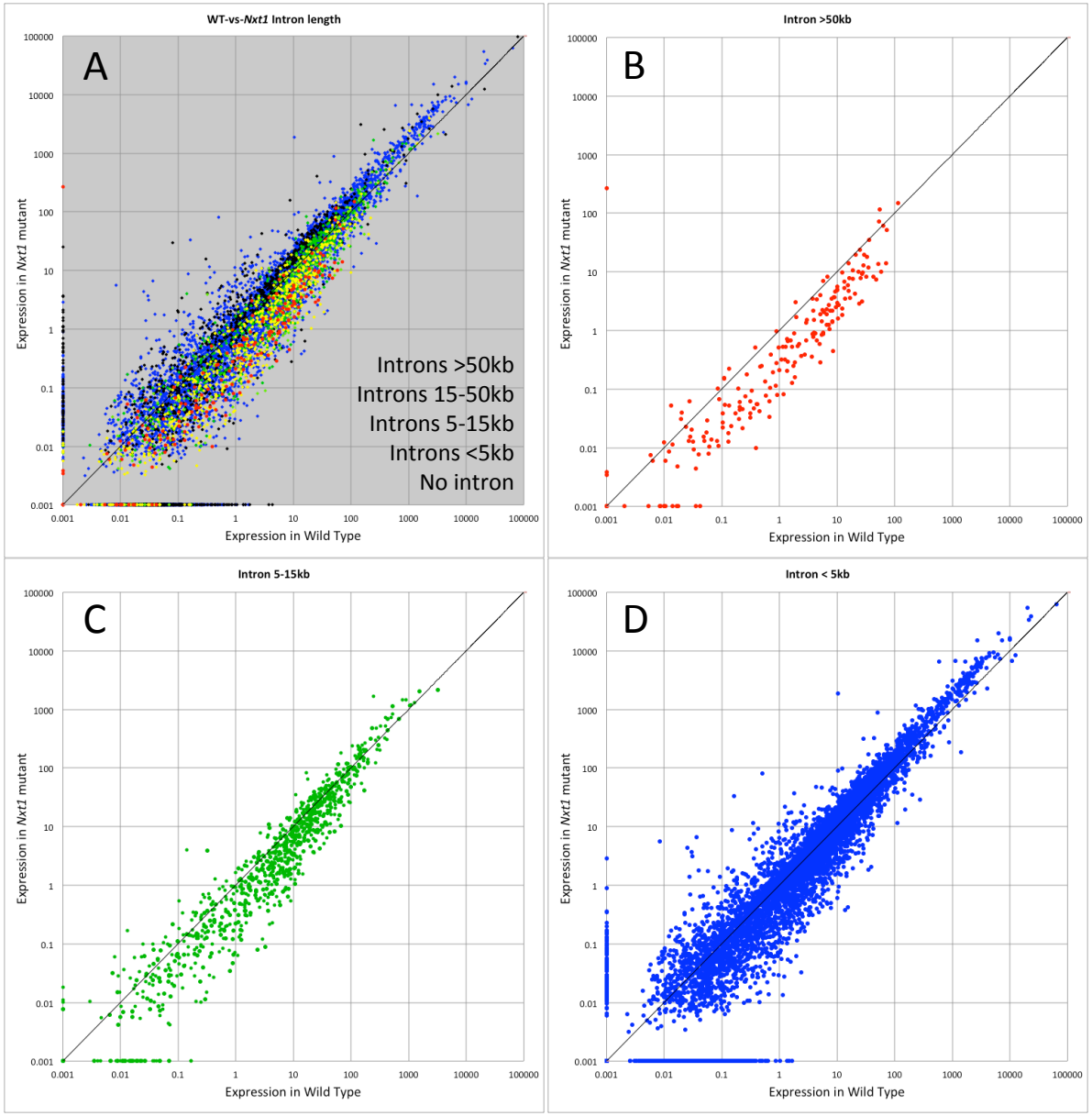
WT-vs-Nxt1 Intron length
A
Introns >50kb
Introns 15-50kb
Introns 5-15kb
Introns <5kb
No intron
Expression in Nxt1 mutant
Expression in Wild Type
Intron >50kb
B
Intron 5-15kb
C
Intron < 5kb
D
0.001
0.01
0.1
1
10
100
1000
10000
100000

# Figure 10

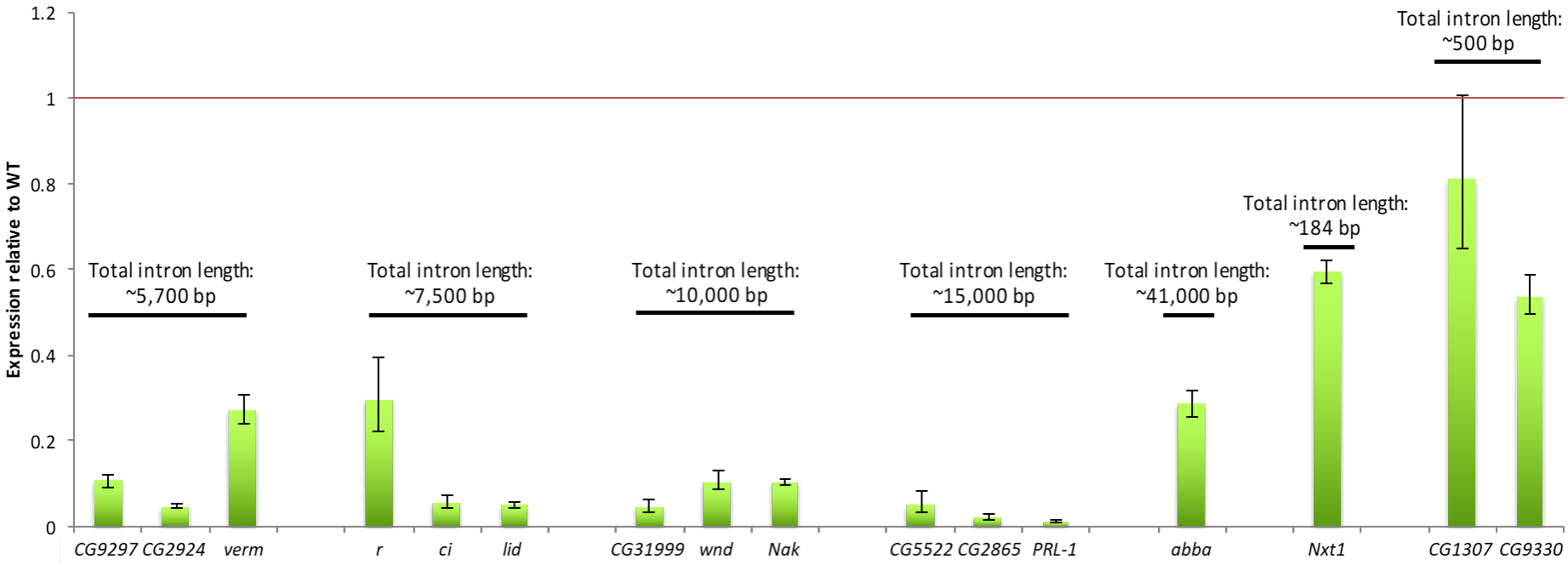
Expression relative to WT
1.2
1
0.8
0.6
0.4
0.2
0
Total intron length: ~5,700 bp
Total intron length: ~7,500 bp
Total intron length: ~10,000 bp
Total intron length: ~15,000 bp
Total intron length: ~41,000 bp
Total intron length: ~184 bp
Total intron length: ~500 bp
CG9297
CG2924
verm
r
ci
lid
CG31999
wnd
Nak
CG5522
CG2865
PRL-1
abba
Nxt1
CG1307
CG9330

# Figure 11

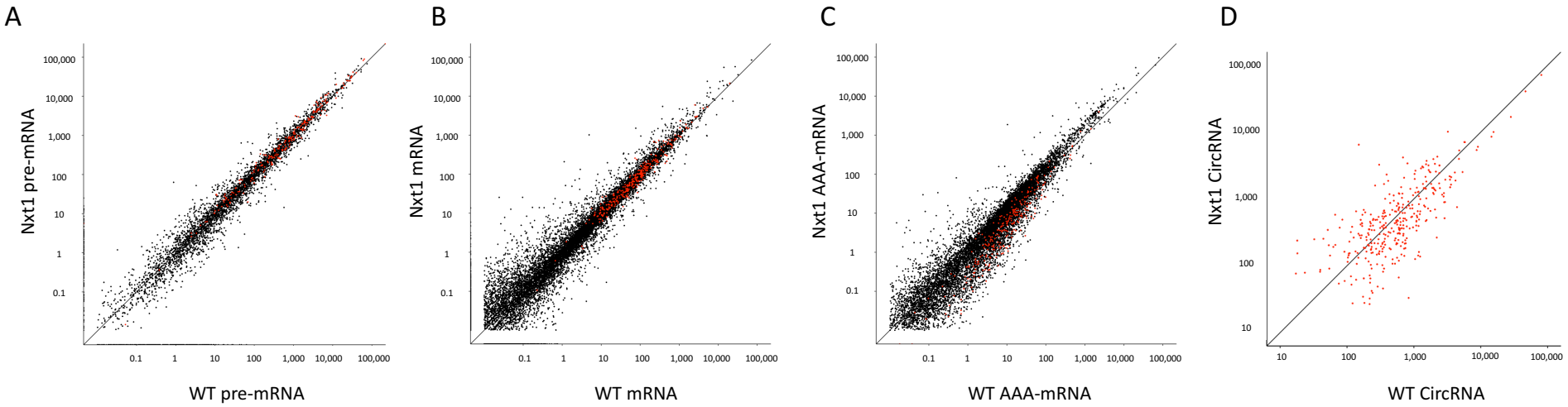
A
Nxt1 pre-mRNA
WT pre-mRNA
B
Nxt1 mRNA
WT mRNA
C
Nxt1 AAA-mRNA
WT AAA-mRNA
D
Nxt1 CircRNA
WT CircRNA

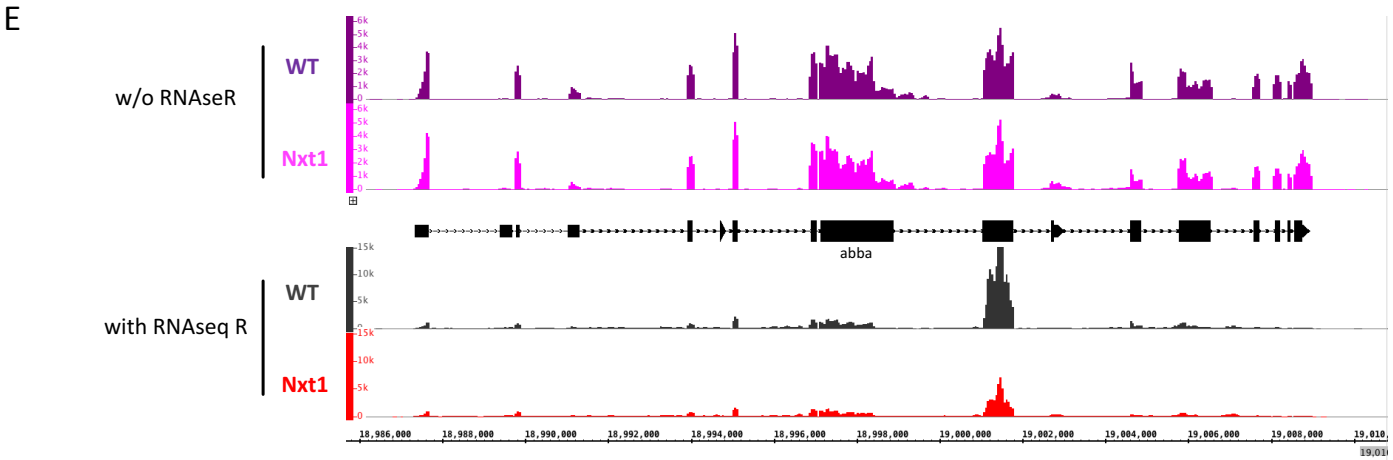
E
w/o RNAseR
WT
Nxt1
with RNAseq R
WT
Nxt1
abba

# Figure 12

A

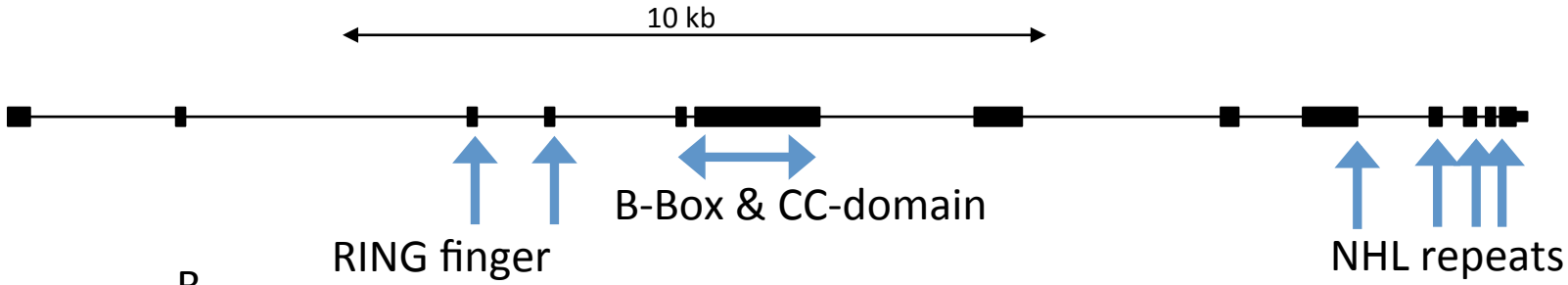


B

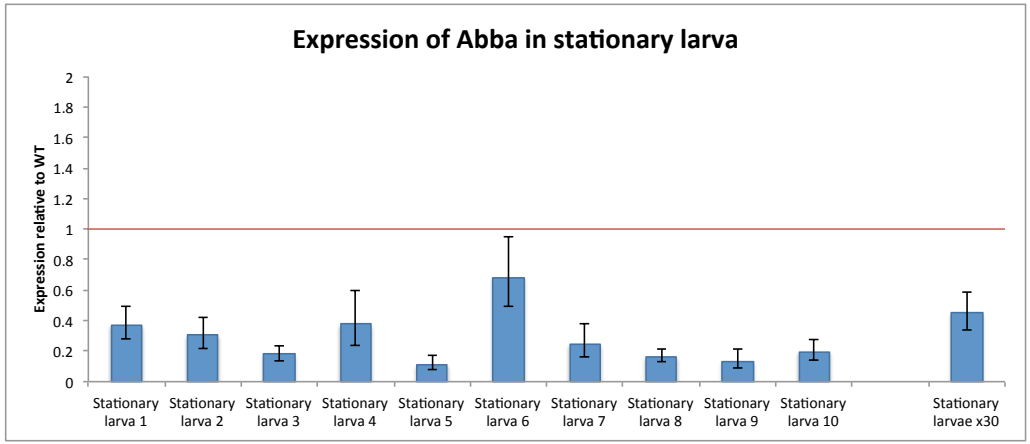


C

*W; Nxt1*$^{DG05102}$/*Nxt1*$^{z2\text{-}0488}$; UAS-Abba$^{fl}$/mef2gal4

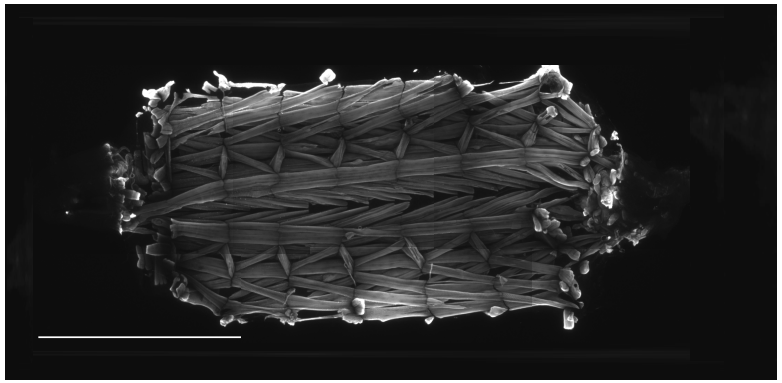

D

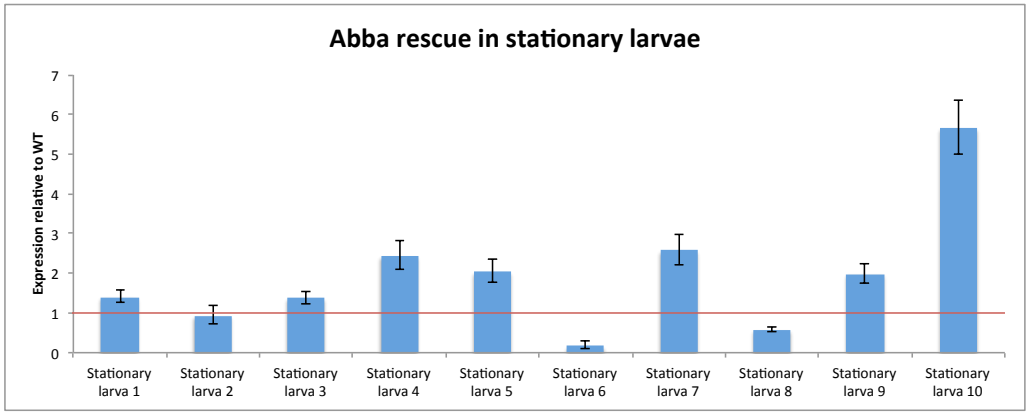

# Table 1

| Median | No. of genes | Total intron length | Number of introns | Smallest intron | Largest intron |
|---|---|---|---|---|---|
| Down-regulated >1.5 fold | **1,821** | 5,769 | 9 | 59 | 2,341 |
| Down-regulated >2 fold | **1,340** | 7,594 | 9 | 59 | 2,931 |
| Down-regulated >4 fold | **567** | 10,201 | 11 | 59 | 3,642 |
| Down-regulated >16 fold | **32** | 15,254 | 10 | 63 | 8,081 |
| **Median** | **No. of genes** | **Total intron length** | **Number of introns** | **Smallest intron** | **Largest intron** |
| Up-regulated >1.5 fold | **1,339** | 368 | 3 | 62 | 160 |
| Up-regulated >2 fold | **572** | 352 | 3 | 62 | 155 |
| Up-regulated >4 fold | **89** | 237 | 2 | 62 | 133 |
| Up-regulated >16 fold | **15** | 238 | 2 | 61 | 180 |
| **Median** | **No. of genes** | **Total intron length** | **Number of introns** | **Smallest intron** | **Largest intron** |
| Non-differentiated | **4,754** | 497 | 4 | 60 | 228 |

# Table 2

| Median | No. of genes | Gene length | No. of transcripts | Shortest transcript | Longest transcript |
|---|---|---|---|---|---|
| Down-regulated >1.5 fold | **1,821** | 8,440 | 3 | 3,220 | 4,263 |
| Down-regulated >2 fold | **1,340** | 9,706 | 3 | 3,301 | 4,533 |
| Down-regulated >4 fold | **567** | 12,162 | 3 | 3,722 | 5,168 |
| Down-regulated >16 fold | **32** | 14,213 | 4 | 3,486 | 5,761 |
| **Median** | **No. of genes** | **Gene length** | **No. of transcripts** | **Shortest transcript** | **Longest transcript** |
| Up-regulated >1.5 fold | **1,339** | 1,584 | 2 | 1.034 | 1,186 |
| Up-regulated >2 fold | **572** | 1,411 | 2 | 901 | 1,027 |
| Up-regulated >4 fold | **89** | 1,353 | 1 | 885 | 994 |
| Up-regulated >16 fold | **15** | 1,411 | 1 | 917 | 1,020 |
| **Median** | **No. of genes** | **Gene length** | **No. of transcripts** | **Shortest transcript** | **Longest transcript** |
| Non-differentiated | **4,754** | 2,496 | 2 | 1,642 | 1,856 |

# Supplementary Figure 1

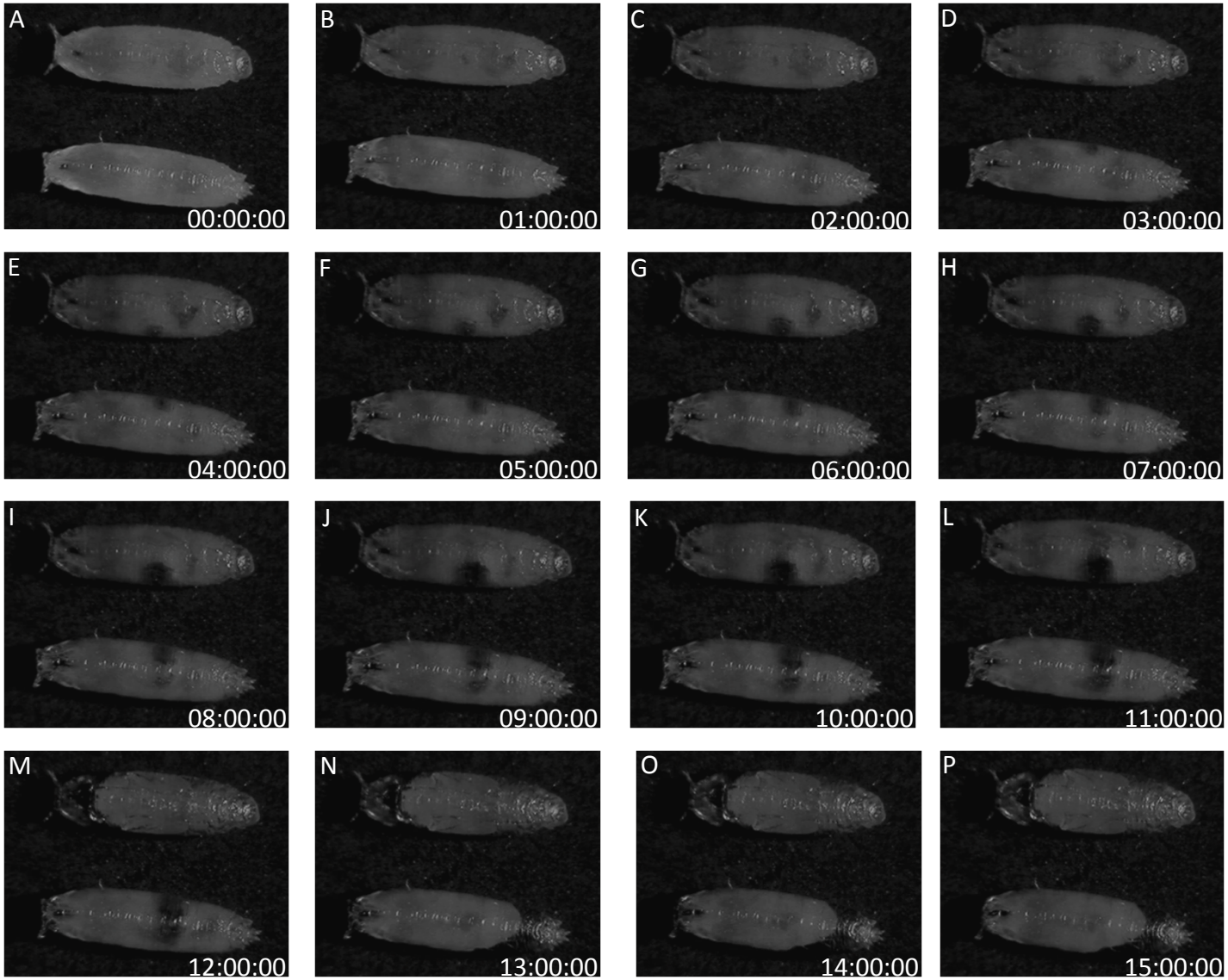

# Supplementary figure 2

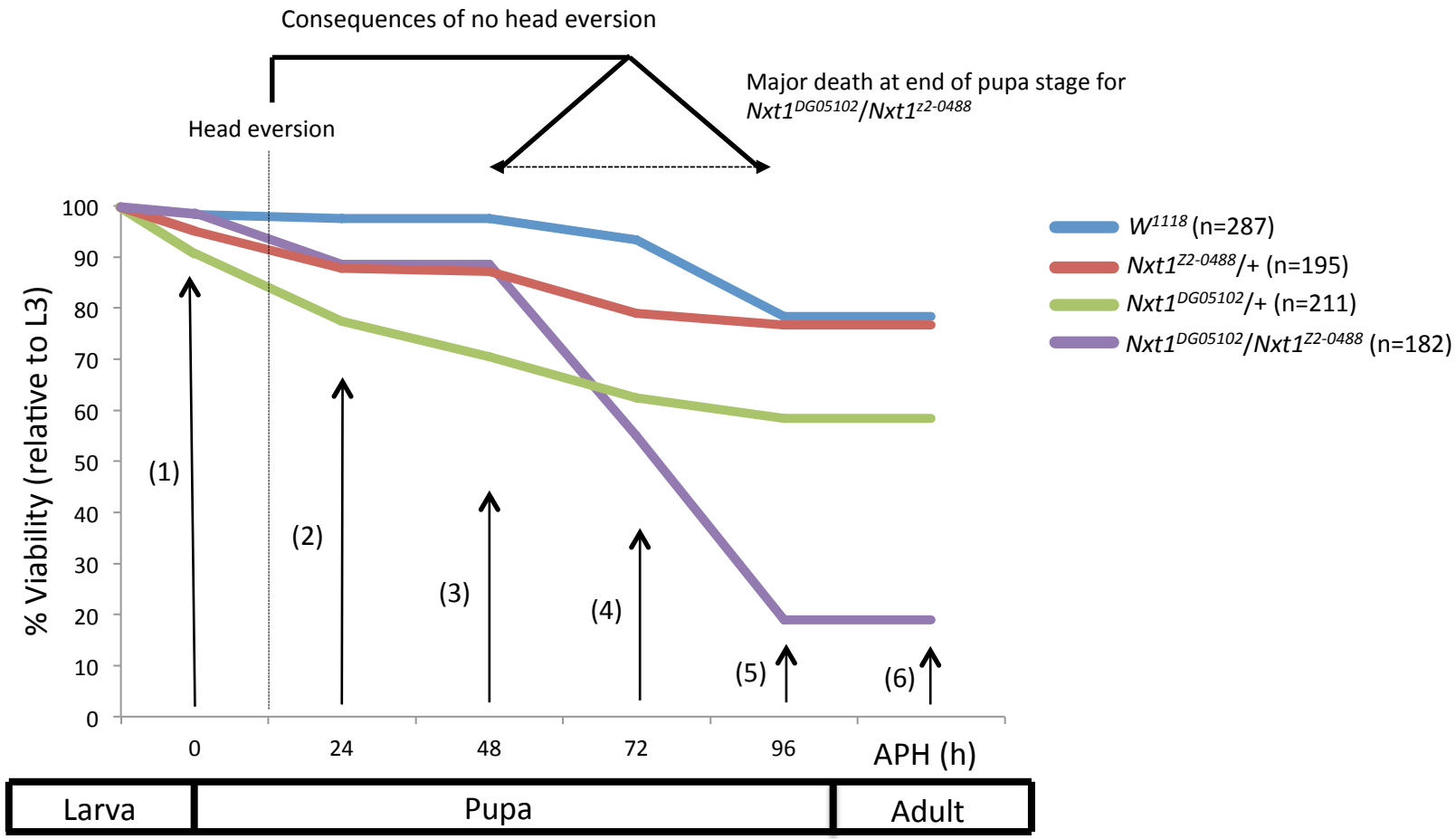


(1): Larvae that did not pupate

(2): No visible development in pupa

(3): Eye starts developing

(4): Bristles on thorax visible

(5): Complete fly development in pupa

(6): Adults that emerged

# Supplementary Fig. 3

A

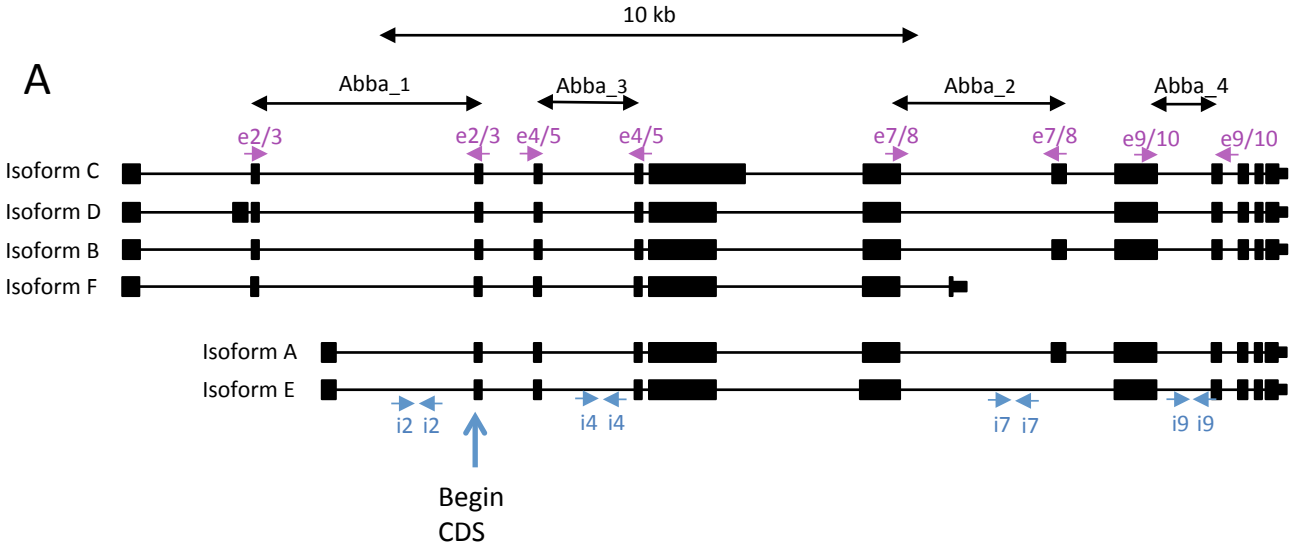


B

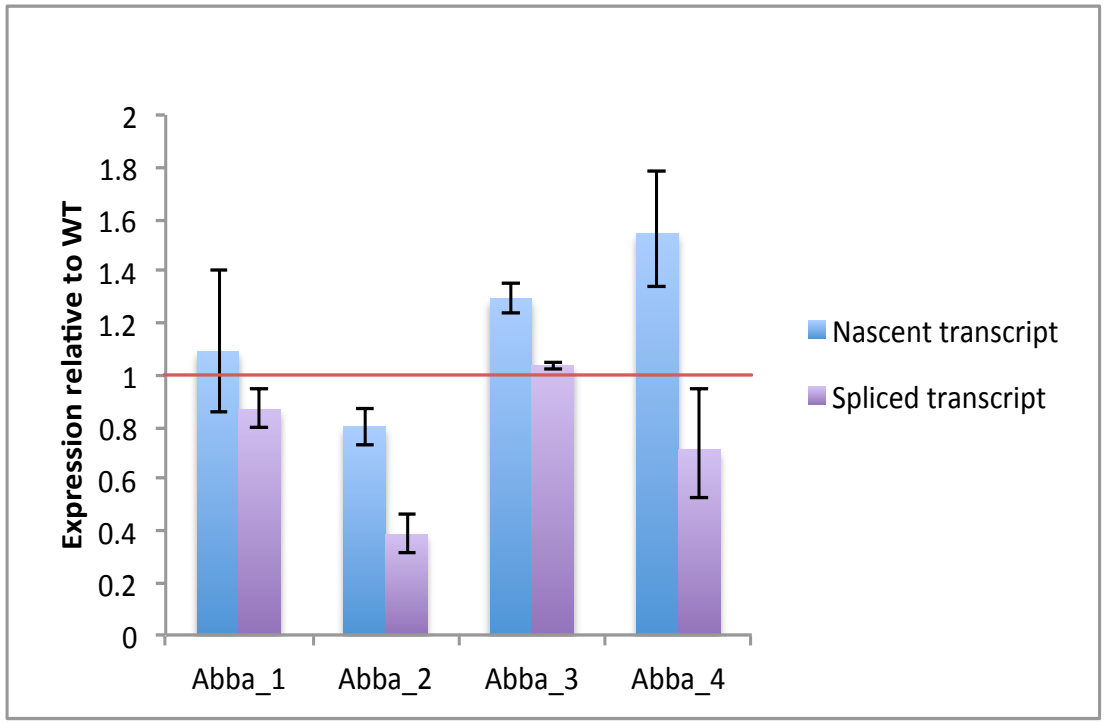

# Supplementary Table 1

| Gene (wandering) | Differentially expressed? | Fold change (log2) | FPKM threshold? | Gene (stationary) | Differentially expressed? | Fold change (log2) | FPKM threshold? | Gene (prepupae) | Differentially expressed? | Fold change (log2) | FPKM threshold? |
|---|---|---|---|---|---|---|---|---|---|---|---|
| ***Br*** | NO | -0.10 | YES | ***Br*** | NO | -0.20 | YES | ***Br*** | NO | +0.02 | YES |
| ***DHR3*** | NO | -0.31 | NO | ***DHR3*** | NO | -0.87 | YES | ***DHR3*** | NO | -0.35 | YES |
| ***EcR*** | NO | -0.08 | YES | ***EcR*** | NO | +0.44 | YES | ***EcR*** | NO | +0.05 | YES |
| ***Usp*** | NO | +0.54 | YES | ***Usp*** | NO | +0.33 | YES | ***Usp*** | NO | -0.14 | YES |
| ***Ecd*** | NO | +0.28 | YES | ***Ecd*** | NO | +0.24 | YES | ***Ecd*** | NO | +0.36 | YES |
| ***Edg78E*** | NO | +0.64 | NO | ***Edg78E*** | NO | +2.15 | NO | ***Edg78E*** | NO | +1.05 | NO |
| ***Edg84A*** | NO | - | - | ***Edg84A*** | NO | - | - | ***Edg84A*** | NO | - | - |
| ***Edg91*** | NO | -0.05 | YES | ***Edg91*** | NO | +0.46 | YES | ***Edg91*** | NO | -0.16 | NO |
| ***Eip55E*** | NO | +0.38 | YES | ***Eip55E*** | NO | +0.30 | YES | ***Eip55E*** | NO | 0.00 | YES |
| ***Eip63E*** | NO | 0.00 | YES | ***Eip63E*** | NO | -0.04 | YES | ***Eip63E*** | NO | +0.36 | YES |
| ***Eip63F-1*** | NO | -0.74 | YES | ***Eip63F-1*** | YES | -0.97 | YES | ***Eip63F-1*** | YES | +1.00 | YES |
| ***Eip63F-2*** | NO | +0.26 | NO | ***Eip63F-2*** | NO | +0.06 | NO | ***Eip63F-2*** | NO | +0.85 | NO |
| ***Eip71CD*** | YES | -0.87 | YES | ***Eip71CD*** | NO | -0.47 | YES | ***Eip71CD*** | NO | -0.18 | YES |
| ***Eip74EF*** | NO | +0.03 | YES | ***Eip74EF*** | NO | 0.00 | YES | ***Eip74EF*** | NO | +0.42 | YES |
| ***Eip75B*** | NO | -0.37 | YES | ***Eip75B*** | NO | -0.49 | YES | ***Eip75B*** | NO | -0.30 | YES |
| ***Eip78C*** | NO | -0.31 | YES | ***Eip78C*** | NO | -0.37 | YES | ***Eip78C*** | YES | +0.68 | YES |
| ***Eip93F*** | NO | +0.35 | NO | ***Eip93F*** | NO | -0.43 | YES | ***Eip93F*** | NO | +0.29 | YES |
| ***Ftz-f1*** | NO | +0.46 | NO | ***Ftz-f1*** | NO | +0.66 | NO | ***Ftz-f1*** | NO | -0.47 | NO |
| ***Eig71Ea*** | NO | -1.18 | YES | ***Eig71Ea*** | YES | -0.57 | YES | ***Eig71Ea*** | NO | +0.32 | YES |
| ***Eig71Eb*** | NO | -1.16 | YES | ***Eig71Eb*** | YES | -1.62 | YES | ***Eig71Eb*** | YES | -0.78 | YES |
| ***Eig71Ec*** | NO | -2.16 | NO | ***Eig71Ec*** | NO | -0.73 | YES | ***Eig71Ec*** | NO | 0.00 | YES |
| ***Eig71Ed*** | NO | -1.27 | YES | ***Eig71Ed*** | YES | -0.93 | YES | ***Eig71Ed*** | YES | -0.42 | YES |
| ***Eig71Ee*** | NO | -0.28 | YES | ***Eig71Ee*** | NO | -0.08 | YES | ***Eig71Ee*** | YES | +0.85 | YES |
| ***Eig71Ef*** | NO | -2.44 | NO | ***Eig71Ef*** | YES | -1.14 | YES | ***Eig71Ef*** | NO | -0.34 | YES |
| ***Eig71Eg*** | NO | -1.99 | YES | ***Eig71Eg*** | YES | -1.55 | YES | ***Eig71Eg*** | YES | -0.97 | YES |
| ***Eig71Eh*** | NO | - | - | ***Eig71Eh*** | NO | -3.34 | NO | ***Eig71Eh*** | YES | -1.48 | YES |
| ***Eig71Ei*** | NO | - | - | ***Eig71Ei*** | NO | -2.50 | NO | ***Eig71Ei*** | NO | -0.75 | YES |
| ***Eig71Ej*** | NO | - | - | ***Eig71Ej*** | NO | - | - | ***Eig71Ej*** | NO | -0.92 | NO |
| ***Eig71Ek*** | NO | - | - | ***Eig71Ek*** | NO | - | - | ***Eig71Ek*** | NO | +1.21 | NO |

# Supplementary. Table 2

| Gene name | Log2 fold change |
|---|---|
| ***abba*** | -0.75 |
| ***up*** | +1.54 |
| ***Arc1*** | +1.84 |
| ***Prm*** | +1.62 |
| ***Mlc2*** | +2.16 |
| ***Mhc*** | +3.02 |
| ***Act57B*** | +2.04 |
| ***mib2*** | -0.48 |
| ***Mlp84B*** | +0.88 |
| ***Actn*** | +0.33 |
| ***Mp20*** | +2.08 |
| ***wupA*** | +0.90 |
| ***sls*** | +0.16 |